

**1<sup>st</sup> International Conference on Innovative Materials  
in Extreme Conditions**



**PROGRAM  
and  
BOOK OF ABSTRACTS**

**22-23 March 2022**

**Belgrade, Serbia**

**1<sup>st</sup> International Conference on Innovative Materials  
in Extreme Conditions**

**PROGRAM  
and  
BOOK OF ABSTRACTS**

**22-23 March 2022**

**Belgrade, Serbia**

**Program and Book of Abstracts of The 1<sup>st</sup> International Conference on Innovative Materials in Extreme Conditions (IMEC2022)** publishes abstracts from the field of material science, physics, chemistry, earth, and computation science on the phenomena arising during the processing and/or exploitation of the innovative materials, which are presented at the international conference on innovative materials in extreme conditions.

***Editors-in-Chief***

Dr. Rer. Nat. Branko Matović

Dr. Ivana Cvijović-Alagić

Dr. Vesna Maksimović

***Publisher***

Vinča Institute of Nuclear Sciences - National Institute of the Republic of Serbia, University of Belgrade

Serbian Society for Innovative Materials in Extreme Conditions (SIM-EXTREME)

***Printing layout***

Dr. Ivana Cvijović-Alagić

Dr. Jelena Erčić

***Press***

Donat Graf d.o.o., Vučka Milićevića 29, 11306 Grocka, Belgrade, Serbia

**ISBN 978-86-7306-158-0**

CIP - Каталогизacija u publikaciji

Народна библиотека Србије, Београд

66.017/.018(048)

INTERNATIONAL CONFERENCE ON INNOVATIVE MATERIALS IN EXTREME  
CONDITIONS

(1 ; 2022 ; BEOGRAD)

Program and book of abstracts / 1st International Conference on Innovative Materials in Extreme Conditions [i. e.] [(IMEC2022)], 22-23 March 2022 Belgrade, Serbia ; [organizers Serbian Society for Innovative Materials in Extreme Conditions [i. e.] (SIM-EXTREME) ... [et al.]] ; [editors-in-chief Branko Matović, Ivana Cvijović-Alagić, Vesna Maksimović]. - Belgrade : University, Vinča Institute of Nuclear Sciences, National Institute of the Republic of Serbia : Serbian Society for Innovative Materials in Extreme Conditions (SIM-EXTREME), 2022 (Belgrade : Donat Graf). - 65 str. : ilustr. ; 30 cm

Str. 3: Preface / editors. - Bibliografija uz pojedine apstrakte.

ISBN 978-86-7306-158-0 (VINS)

а) Наука о материјалима -- Апстракти б)

Технички материјали -- Апстракти

COBISS.SR-ID 60606985

-----

## **Preface**

*Dear conference participants and readers, we have the pleasure to welcome you all to Belgrade, Serbia as the venue for the 1<sup>st</sup> International Conference on Innovative Materials in Extreme Conditions (IMEC2022). This event is jointly organized by the Serbian Society for Innovative Materials in Extreme Conditions (SIM-EXTREME), the Center of Excellence "Center for Synthesis, Processing and Characterization of Materials for Application in Extreme Conditions - CEXTREME LAB", University of Belgrade, the Faculty of Science and Mathematics, University of Niš, and the Faculty of Mechanical Engineering, University of Belgrade.*

*The scope of the IMEC2022 is to become the worldwide forum for discussion of experts and young researchers on the phenomena arising during the processing and/or exploitation of the innovative materials. The IMEC2022 conference is focused on the current research in the field of material science, physics, chemistry, earth, and computation science. Experimental and computational investigations of materials obtained or operated under extreme conditions presented during the conference are highlighting recent progress in the development of the innovative materials at high pressures, under high magnetic and electric fields, over a wide range of temperatures, radiation conditions, corrosive environments, under extreme mechanical loads and non-equilibrium thermodynamic conditions. The interrelation between external effects, microstructural characteristics, and material properties is considered on the experimental and theoretical level to obtain new or enhanced insights into the material behavior and their application.*

*We want to use this opportunity to thank our sponsors and co-organizers for helping us to successfully organize the IMEC2022 conference. First of all, we want to mention that the Ministry of Education, Science and Technological Development of the Republic of Serbia recognized our conference as an important event and gave their financial endorsement. Also, we want to thank the Vinča Institute of Nuclear Sciences – National Institute of the Republic of Serbia, University of Belgrade, for their strong financial support. In the end, we would like to thank all the members of the Conference Advisory Board, the Conference International Scientific Committee, and the Conference Organizing Committee who participated in the preparations of the IMEC2022 conference.*

*Editors*

## ORGANIZERS



*Serbian Society for Innovative Materials in Extreme Conditions (SIM-EXTREME)*



*Center of Excellence "Center for Synthesis, Processing and Characterization of Materials for Application in Extreme Conditions" (CEXTREME LAB), Vinča Institute of Nuclear Sciences - National Institute of the Republic of Serbia, University of Belgrade*



*Faculty of Science and Mathematics, University of Niš*



*Faculty of Mechanical Engineering, University of Belgrade*

## SPONSORS



*Vinča Institute of Nuclear Sciences - National Institute of the Republic of Serbia,  
University of Belgrade*



*Ministry of Education, Science and Technological Development of the Republic of Serbia*

### ***Chair***

---

Prof. Dr. Rer. Nat. Branko Matović *Center of Excellence “CEXTREME LAB”, Vinča Institute of Nuclear Sciences, University of Belgrade, Serbia*

### ***Advisory Board***

---

Prof. Dr. Rer. Nat. N.V. Ravi Kumar *Indian Institute of Technology Madras, India*

Dr. Miladin Radović *Department of Materials Science and Engineering, Texas A&M University, USA*

Assoc. Prof. Dr. Claus Rebholz *Department of Mechanical and Manufacturing Engineering, University of Cyprus, Cyprus*

Prof. Gordana Bakić *Faculty of Mechanical Engineering, University of Belgrade*

Prof. Vladimir Ivanov *Russian Academy of Sciences (RAS), Kurnakov Institute of General and Inorganic Chemistry, Russian Federation*

Prof. Pavol Šajgalik *Institute of Inorganic Chemistry, Slovak Academy of Sciences, Slovak Republic*

Prof. Dr. Zoran Popović *Serbian Academy of Science and Art (SASA), Serbia*

Prof. Pei-Zhong Feng *School of Materials Science and Engineering, China University of Mining and Technology, PR China*

Prof. Lidija Ćurković *Faculty of Mechanical Engineering and Naval Architecture, University of Zagreb, Croatia*

Dr. Vladimir Urbanovich *Centre of Science and Practice of Materials, National Academy of Sciences of Belarus, Belarus*

### ***International Scientific Committee***

---

Dr. Tetiana Prikhna *V. Bakul Institute for Superhard Materials, National Academy of Sciences of Ukraine, Ukraine*

Dr. Enikő Volceanov *Metallurgical Research Institute, Politehnica University of Bucharest, Romania*

Dr. Peter Tatarko *Institute of Inorganic Chemistry, Slovak Academy of Sciences, Slovak Republic*

Prof. Michele Cali *Electric, Electronics and Computer Engineering Department, University of Catania, Italia*

Prof. Dr. Branislav Jelenković *Serbian Academy of Science and Art (SASA), Serbia*

Dr. Ivana Cvijović-Alagić *Center of Excellence “CEXTREME LAB”, Vinča Institute of Nuclear Sciences, University of Belgrade, Serbia*

Dr. Vesna Maksimović *Center of Excellence “CEXTREME LAB”, Vinča Institute of Nuclear Sciences, University of Belgrade, Serbia*

PD Dr. Rer. Nat. Emanuel Ionescu *Fraunhofer-Einrichtung für Wertstoffkreisläufe und Ressourcenstrategie IWKS, Germany*

Dr. Jelena Zagorac *Center of Excellence “CEXTREME LAB”, Vinča Institute of Nuclear Sciences, University of Belgrade, Serbia*

Prof. Aleksandra Zarubica *Faculty of Science and Mathematics, University of Niš*

Prof. Miloš Đukić *Faculty of Mechanical Engineering, University of Belgrade*

***Organizing Committee***

---

Dr. Rer. Nat. Dejan Zagorac	<i>Center of Excellence “CEXTREME LAB”, Vinča Institute of Nuclear Sciences, University of Belgrade, Serbia</i>
Dr. Jelena Stašić	<i>Center of Excellence “CEXTREME LAB”, Vinča Institute of Nuclear Sciences, University of Belgrade, Serbia</i>
Dr. Tamara Minović Arsić	<i>Center of Excellence “CEXTREME LAB”, Vinča Institute of Nuclear Sciences, University of Belgrade, Serbia</i>
Dr. Marija Prekajski Đorđević	<i>Center of Excellence “CEXTREME LAB”, Vinča Institute of Nuclear Sciences, University of Belgrade, Serbia</i>
Dr. Maria Čebela	<i>Center of Excellence “CEXTREME LAB”, Vinča Institute of Nuclear Sciences, University of Belgrade, Serbia</i>
Dr. Marjan Randelović	<i>Faculty of Science and Mathematics, University of Niš</i>
Dr. Filip Veljković	<i>Vinča Institute of Nuclear Sciences, University of Belgrade</i>
Vladimir Pavkov	<i>Center of Excellence “CEXTREME LAB”, Vinča Institute of Nuclear Sciences, University of Belgrade, Serbia</i>

***Scientific Secretary***

---

Dr. Jelena Erčić	<i>Center of Excellence “CEXTREME LAB”, Vinča Institute of Nuclear Sciences, University of Belgrade, Serbia</i>
------------------	---



## TABLE OF CONTENTS

<b>PROGRAM</b> .....	13
22 <sup>nd</sup> March 2022 .....	14
23 <sup>rd</sup> March 2022 .....	16
<b>PLENARY LECTURES</b> .....	17
<i>Peter Tatarko, Hakan Ünsal, Alexandra Kovalčíková, Branko Matović, Zdeněk Chlup, Monika Tatarková, Michal Hičák, Ivo Dlouhý</i> Ultra-high temperature ceramics with improved ablation resistance .....	18
<i>Ravi Kumar</i> Design & development of precursor-derived ultra-high temperature resistant ceramic coatings and fibres for space applications .....	19
<i>Ivana Cvijović-Alagić, Slađana Laketić, Miloš Momčilović, Jovan Ciganović, Đorđe Veljović, Marko Rakin</i> Laser irradiation as an easy-to-apply method for Ti-based implant materials enhancement .....	20
<i>Dejan Zagorac</i> Innovative materials under extreme conditions: Multidisciplinary approach on multiscale level .....	21
<b>INVITED LECTURES and ORAL PRESENTATIONS</b> .....	22
<i>Zoltán Lenčేశ, Mohamed Radwan, Patrícia Petrisková, Adriana Czímerová, Peter Boháč, Pavol Šajgalík</i> Spinel-based ceramics for LEDs and photocatalytic applications .....	23
<i>Michal Hičák, Miroslav Hnatko, Zoltán Lenčేశ, Pavol Šajgalík</i> Surface modification of Si <sub>3</sub> N <sub>4</sub> -Y <sub>2</sub> O <sub>3</sub> composites – optimisation of oxyacetylene torch conditions .....	24
<i>Gordana Bakić, Milos Djukic, Bratislav Rajicic, Aleksandar Maslarevic, Vesna Maksimovic, Vladimir Pavkov, Nenad Milosevic</i> High Temperature Failures of Metals .....	25

<i>Miloš Đukić, Gordana M. Bakic, Vera Sijacki Zeravcic, Bratislav Rajcic, Aleksandar Sedmak, Muhammad Wasim, Jovana Perisic</i>	
Hydrogen embrittlement mechanisms in steels at different length scales .....	26
<i>Ondrej Hanzel, Zoltán Lenčes, Young-Wook Kim, Ján Fedor, Pavol Šajgalík</i>	
Silicon carbide - graphene composites with high functional properties .....	27
<i>Hakan Ünsal, Ondrej Hanzel, Salvatore Grasso, Alexandra Kovalčíková, Ivo Dlouhý, Peter Tatarko</i>	
Preparation and characterization of B <sub>4</sub> C/TiB <sub>2</sub> composites .....	28
<i>Branko Matović, Marija Prekajski Djordjevic, Marko Nikolic</i>	
Luminescence properties of Eu <sup>3+</sup> doped Mayenite under high pressure .....	29
<i>Jelena Maletaškić, Joshua Emory, Anna Gubarevich, Liao Nengqing, Katsumi Yoshida</i>	
Development of Highly Microstructure-Controlled Alumina Ceramics .....	30
<i>Vesna Maksimović, Nebojša Nikolić</i>	
Electrodeposition of powders in vigorous hydrogen evolution conditions .....	31
<i>Marjan Ranđelović, Aleksandra Zarubica, Branko Matović</i>	
Supercritical Hydrothermal Synthesis of ceramic powders in batch conditions .....	32
<i>Matej Fonović, Lovro Liverić, Neven Tomašić, Zoran Knežević</i>	
Layer formation on ternary Ni-10Cr-1Si (in wt.%) alloy upon low temperature gaseous nitriding .....	33
<i>Jelena Zagorac, Christian J. Schön, Dušica Jovanović, Dejan Zagorac, Tamara Škundrić, Milan Pejić, Branko Matović</i>	
Predicting stable modifications of Ce <sub>2</sub> ON <sub>2</sub> using a combination of global optimization and data mining .....	34
<i>Milovan Stoiljković, Suzana Veličković, Filip Veljković, Đorđe Kapuran</i>	
Generation of a laser-supported detonation (LSD) wave .....	35
<i>Zoran Jovanović, Andrzej Olejniczak, Nina Daneu, Matjaž Spreitzer, Danica Bajuk-Bogdanović, Željko Mravik, Vladimir Skuratov</i>	
The Effects of Swift Heavy Ion Irradiation on Structural Properties of Glassy Carbon ....	36
<i>Manuel Gruber, Walter Harrer, Raul Bermejo, Anton Tilz, Wolfgang Fimml, Andreas Wimmer</i>	
Ceramic Spark Plug Electrodes for Large Gas Engine Applications .....	37
<i>Branislav Jelenković</i>	
Ultra fast laser processing of materials for science and industry .....	38
<i>Claus Rebholz, Nikolaos Kostoglou, Branko Matovic</i>	
Thermal and chemical stability of boron nitride nanostructures .....	39

<i>Marija Prekajski Đorđević, Branko Matović, Jelena Maletaškić, Jelena Erčić, R. Subasri</i> Sintering properties of heavily Bi-doped CeO <sub>2</sub> .....	40
<b>POSTER PRESENTATIONS .....</b>	<b>41</b>
<i>Bratislav Todorović, Pavle I. Premović, Dragan T. Stojiljković, Sreten B. Stojanović</i> ESR analysis of Mn <sup>2+</sup> cations at temperatures of 4.2-293 K in kerogen isolated from graptolitic black shale at Zvonačka Banja (Zvonce, Eastern Serbia) .....	42
<i>Dejan Zagorac, Ivana Cvijović-Alagić, Jelena Zagorac, Svetlana Butulija, Jelena Erčić, Ondrej Hanzel, Richard Sedlák, Maksym Lisnichuk, Tamara Škundrić, Milan Pejić, Dušica Jovanović, Peter Tatarko, Branko Matović</i> DFT study of structural stability and mechanical properties: High-Entropy Alloys (HEAs) - Ultra-High Temperature Ceramics (UHTC) .....	43
<i>Dušica Jovanović, Jelena Zagorac, Dejan Zagorac, Branko Matović</i> Structural, electronic and mechanical properties of bulk B <sub>4</sub> C from first principles .....	44
<i>Dušica Jovanović, Dejan Zagorac, Branko Matović, Milan Pejić, Tamara Škundrić, Jelena Zagorac</i> Anion substitution and the structure-property influence of sulfur on mixed TiO <sub>2</sub> /TiS <sub>2</sub> compounds .....	45
<i>Filip Veljković, Branko Matovic, Svetlana Butulija, Milovan Stoilkovic, Ivana Stajcic, Bojan Jankovic, Suzana Velickovic</i> Laser desorption/ionization mass spectrometry of Li <sub>1.999</sub> Ta <sub>0.005</sub> SiO <sub>3</sub> .....	46
<i>Jelena Erčić, Dejan Zagorac, Olga Ivanova, Alexander Baranchikov, Taisiya Shekunova, Khursand Yorov, Olga Gajtko, Lili Yang, Marina Rumyantseva, Vladimir Ivanov, Branko Matović</i> Hydrogen peroxide-assisted route for nanocrystalline WO <sub>3</sub> synthesis with excellent sensing response .....	47
<i>Jelena Zagorac, Dušica Jovanović, Dejan Zagorac, Tamara Škundrić, Milan Pejić, Branko Matović</i> Crystal structure and properties of theoretically predicted c-AlB <sub>12</sub> .....	48
<i>Ivana Ropuš, Lidija Ćurković, Sanda Rončević, Ivana Gabelica</i> Influence of temperature on corrosion of high purity alumina ceramics in acidic aqueous solution .....	49
<i>Tijana Stamenković, Nadežda Radmilović, Maria Čebela, Marija Prekajski-Dorđević, Vesna Lojpur</i> Investigation of Yb <sup>3+</sup> /Er <sup>3+</sup> doped SrGd <sub>2</sub> O <sub>4</sub> up-conversion nanomaterial obtained via combustion synthesis .....	50

<b><i>Tijana Stamenković, Nadežda Radmilović, Jelena Erčić, Maria Čebela, Vesna Lojpur</i></b> Synthesis and characterization of a new Dy <sup>3+</sup> and Sm <sup>3+</sup> doped SrGd <sub>2</sub> O <sub>4</sub> down-conversion nanomaterial obtained via glycine-assisted combustion synthesis .....	51
<b><i>Maria Čebela, Milena Rosić, Vesna Lojpur</i></b> Mechanochemical activation of starting oxide mixtures for solid-state synthesis of BiFeO <sub>3</sub>	52
<b><i>Milan Pejić, Dejan Zagorac, Jelena Zagorac, Tamara Škundrić, Dušica Jovanović, Branko Matović</i></b> Energy landscape and crystal structure investigations of holmium(III) fluoro-selenide HoFSe .....	53
<b><i>Milan Pejić, Dejan Zagorac, Jelena Zagorac, Tamara Škundrić, Dušica Jovanović, Branko Matović</i></b> Theoretical study of ground state properties of Na <sup>+</sup> , Cs <sup>+</sup> , Mg <sup>2+</sup> and Ba <sup>2+</sup> doped mayenite and its electride forms under extreme conditions .....	54
<b><i>Milan Vukšić, Irena Žmak, Lidija Čurković</i></b> Conventional and Unconventional Sintering of Alumina Ceramics .....	55
<b><i>Radojka Vujasin, Ksenija Kumrić, Aleksandar Devečerski, Mia Omerašević, Marija Egerić, Đorđe Petrović, Ljiljana Matović</i></b> Water under extreme conditions: simultaneous gamma irradiation/carbon char adsorption resulted in improved methylene blue degradation .....	56
<b><i>Sonja Jovanović, Marija Grujičić, Marko Jelić, Marija Vukomanović, Matjaž Spreitzer, Marjeta Maček-Kržmanc, Davide Peddis</i></b> Solvochemical synthesis of zinc- and gallium-substituted cobalt ferrite nanoparticles .....	57
<b><i>Svetlana Butulija, Jelena Maletaškić, Bratislav Todorović, Sanja Petrović, Aleksandra Dapčević, Branko Matović</i></b> Heavily Pb-doped Ce-solid solutions .....	58
<b><i>Tamara Škundrić, Dejan Zagorac, Johann Christian Schön, Jelena Zagorac, Milan Pejić, Dušica Jovanović, Branko Matović</i></b> Crystal structure prediction of novel Cr <sub>2</sub> SiN <sub>4</sub> compound under extreme conditions .....	59
<b><i>Tamara Škundrić, Dejan Zagorac, Aleksandra Zarubica, Jelena Zagorac, Milan Pejić, Dušica Jovanović, Peter Tatarko, Branko Matović</i></b> Mechanical and elastic properties of SiB <sub>6</sub> : Theoretical investigations through ab initio calculations .....	60
<b><i>Vladimir Pavkov, Gordana Bakić, Vesna Maksimović, Miloš Đukić, Bratislav Rajičić, Aleksandar Maslarević, Branko Matović</i></b> Damage to a tube of output reheater due to gas corrosion .....	61

*Nadežda Radmilović, Tijana Stamenković, Vesna Lojpur*

Influence of host lattice on luminescence properties of up-conversion  $\text{Ln}_2\text{MoO}_6$  (Ln=Y, Gd) powders co-doped with  $\text{Er}^{3+}/\text{Yb}^{3+}$  synthesised at high temperatures ..... 62

**AUTHOR INDEX** ..... 63

# **PROGRAM**

22<sup>nd</sup> March 2022

<b>9:00 – 16:00</b>	<b>Conference registration</b> (Exhibition hall)
<b>9:00</b>	<b>Conference opening and Welcome address</b> <i>Branko Matović, Conference Chair</i>
<b>SESSION A</b>	
<b>Session Chairs:</b> <i>Branko Matović, University of Belgrade, Serbia</i> <i>Pavol Šajgalik, Slovak Academy of Sciences, Slovakia</i>	
<b>9:10 – 9:40</b>	<b>Plenary Lecture</b> <i>Peter Tatarko, Slovak Academy of Sciences, Slovakia</i> Ultra-high temperature ceramics with improved ablation resistance
<b>9:40 – 10:00</b>	<i>Zoltán Lenčేశ, Slovak Academy of Sciences, Slovakia</i> Spinel-based ceramics for LEDs and photocatalytic applications
<b>10:00 – 10:20</b>	<i>Michal Hičák, Slovak Academy of Sciences, Slovakia</i> Surface modification of Si <sub>3</sub> N <sub>4</sub> -Y <sub>2</sub> O <sub>3</sub> composites – optimisation of oxyacetylene torch conditions
<b>10:20 – 10:40</b>	<i>Gordana Bakić, University of Belgrade, Serbia</i> High Temperature Failures of Metals
<b>10:40 – 11:00</b>	<i>Miloš Đukić, University of Belgrade, Serbia</i> Hydrogen embrittlement mechanisms in steels at different length scales
<b>11:00 – 12:00</b>	<b>Poster Session</b> (Exhibition hall)
<b>11:00 – 11:30</b>	<b>Coffee break</b> (Exhibition hall)
<b>SESSION B</b>	
<b>Session Chairs:</b> <i>Ravi Kumar, Indian Institute of Technology Madras, India</i> <i>Lidija Čurković, University of Zagreb, Croatia</i>	
<b>11:30 – 11:50</b>	<i>Ondrej Hanzel, Slovak Academy of Sciences, Slovakia</i> Silicon carbide - graphene composites with high functional properties
<b>11:50 – 12:10</b>	<i>Hakan Ünsal, Slovak Academy of Sciences, Slovakia</i> Preparation and characterization of B <sub>4</sub> C/TiB <sub>2</sub> composites
<b>12:10 – 12:20</b>	<i>Branko Matović, University of Belgrade, Serbia</i> Luminescence properties of Eu <sup>3+</sup> doped mayenite under high pressure
<b>12:20 – 12:40</b>	<i>Jelena Maletaškić, University of Belgrade, Serbia</i> Development of Highly Microstructure-Controlled Alumina Ceramics

<b>12:40 – 13:00</b>	<i>Vesna Maksimović, University of Belgrade, Serbia</i> Electrodeposition of powders in vigorous hydrogen evolution conditions
<b>13:00 – 14:30</b>	<b>Lunch break</b> (Conference venue)
<b>SESSION C</b>	
<b>Session Chairs:</b> <i>Zoltán Lenčéš, Slovak Academy of Sciences, Slovakia</i> <i>Claus Rebholz, University of Cyprus, Cyprus</i>	
<b>14:30 – 15:00</b>	<b>Plenary Lecture</b> <i>Ravi Kumar, Indian Institute of Technology Madras, India</i> Design & development of precursor-derived ultra-high temperature resistant ceramic coatings and fibres for space applications
<b>15:00 – 15:20</b>	<i>Marjan Randelović, University of Niš, Serbia</i> Supercritical Hydrothermal Synthesis of ceramic powders in batch conditions
<b>15:20 – 15:40</b>	<i>Matej Fonović, University of Rijeka, Croatia</i> Layer formation on ternary Ni-10Cr-1Si (in wt.%) alloy upon low temperature gaseous nitriding
<b>15:40 – 16:00</b>	<i>Jelena Zagorac, University of Belgrade, Serbia</i> Predicting stable modifications of Ce <sub>2</sub> ON <sub>2</sub> using a combination of global optimization and data mining
<b>20:00</b>	<b>Conference gala dinner</b> Mezestoran Dvorište, <i>Address</i> : Svetogorska 46, Belgrade



23<sup>rd</sup> March 2022

<b>SESSION D</b>	
<b>Session Chairs:</b> <i>Peter Tatarko, Slovak Academy of Sciences, Slovakia</i> <i>Branislav Jelenković, Serbian Academy of Sciences and Arts, Serbia</i>	
<b>9:30 – 10:00</b>	<b>Plenary Lecture</b> <i>Ivana Cvijović-Alagić, University of Belgrade, Serbia</i> Laser irradiation as an easy-to-apply method for Ti-based implant materials enhancement
<b>10:00 – 10:20</b>	<i>Milovan Stoiljković, University of Belgrade, Serbia</i> Generation of a laser-supported detonation (LSD) wave
<b>10:20 – 10:40</b>	<i>Zoran Jovanović, University of Belgrade, Serbia</i> The Effects of Swift Heavy Ion Irradiation on Structural Properties of Glassy Carbon
<b>10:40 – 11:00</b>	<i>Manuel Gruber, Montanuniversität Leoben, Austria</i> Ceramic Spark Plug Electrodes for Large Gas Engine Applications
<b>11:00 – 12:00</b>	<b>Poster Session</b> (Exhibition hall)
<b>11:00 – 11:30</b>	<b>Coffee break</b> (Exhibition hall)
<b>SESSION E</b>	
<b>Session Chairs:</b> <i>Branko Matović, University of Belgrade, Serbia</i> <i>Ivana Cvijović-Alagić, University of Belgrade, Serbia</i>	
<b>11:30 – 12:00</b>	<b>Plenary Lecture</b> <i>Dejan Zagorac, University of Belgrade, Serbia</i> Innovative materials under extreme conditions: Multidisciplinary approach on multiscale level
<b>12:00 – 12:20</b>	<i>Branislav Jelenković, Serbian Academy of Sciences and Arts, Serbia</i> Ultra fast laser processing of materials for science and industry
<b>12:20 – 12:40</b>	<i>Claus Rebholz, University of Cyprus, Cyprus</i> Thermal and chemical stability of boron nitride nanostructures
<b>12:40 – 13:00</b>	<i>Marija Prekajski Đorđević, University of Belgrade, Serbia</i> Sintering properties of heavily Bi-doped CeO <sub>2</sub>
<b>13:00 – 15:00</b>	<b>Lunch break</b> (Conference venue)
<b>16:00 – 17:00</b>	<b>Guided visit to National Museum in Belgrade</b> <i>Address: Trg republike 1a, Belgrade</i>

# **PLENARY LECTURES**

## Ultra-high temperature ceramics with improved ablation resistance

**Peter Tatarko<sup>1</sup>, Hakan Ünsal<sup>1</sup>, Alexandra Kovalčíková<sup>2</sup>, Branko Matović<sup>3</sup>, Zdeněk Chlup<sup>4</sup>,  
Monika Tatarková<sup>1</sup>, Michal Hičák<sup>1</sup>, Ivo Dlouhý<sup>4</sup>**

<sup>1</sup>*Institute of Inorganic Chemistry, Slovak Academy of Sciences, Dubravska cesta 9, 845 36  
Bratislava, Slovakia*

<sup>2</sup>*Institute of Materials Research, Slovak Academy of Sciences, Watsonova 47, 040 01 Kosice,  
Slovakia*

<sup>3</sup>*Centre of Excellence-CextremeLab, Vinča Institute of Nuclear Sciences, University of Belgrade,  
Mike Petrovica-Alasa 12-14, 11000 Belgrade, Serbia*

<sup>4</sup>*Institute of Physics of Materials, Academy of Sciences of the Czech Republic, Žitkova 22, 616 62,  
Brno, Czech Republic*

The effect of different rare-earth oxide additives ( $\text{Lu}_2\text{O}_3$ ,  $\text{Yb}_2\text{O}_3$  and  $\text{Eu}_2\text{O}_3$ ) on the sintering, microstructure evolution, phase composition and mechanical properties of  $\text{ZrB}_2 - 25\text{vol. \% SiC}$  ultra-high temperature ceramics was investigated. No significant effect of different rare-earth oxides on the room temperature properties (hardness, fracture toughness, Young's modulus, flexural strength) was observed. On the other hand, the ablation resistance of the materials up to  $\sim 2700^\circ\text{C}$  was significantly improved (by  $\sim 30\%$ ) when the  $\text{Yb}_2\text{O}_3$  additive was used. The improved ablation resistance was attributed to the in-situ formation of  $\text{Yb}_2\text{Zr}_2\text{O}_7$  pyrochlore phase on the surface of the materials during the ablation tests. Therefore, this additive was selected for further investigation. The effect of various amounts of  $\text{Yb}_2\text{O}_3$  and  $\text{Yb}_2\text{Zr}_2\text{O}_7$  additives (2, 5, and 10 wt.%) on the densification, room temperature mechanical properties and ablation resistance of  $\text{ZrB}_2 - 25\text{vol. \% SiC}$  composites prepared by two different approaches (reactive SPS sintering vs. non-reactive SPS sintering) was investigated. The use of reactive SPS approach helped to significantly decrease the sintering temperature from  $2000^\circ\text{C}$  to  $1600^\circ\text{C}$ . At the same time, the lower temperature and the in-situ formation of phases resulted in a significantly finer microstructure of  $\text{ZrB}_2 - 25\text{vol. \% SiC}$  when sintered by reactive approach. This led to the improved room temperature mechanical properties and the ablation resistance of the materials. No significant deterioration of the room temperature properties was observed even after the addition of 10 wt.% of  $\text{Yb}_2\text{O}_3$  and  $\text{Yb}_2\text{Zr}_2\text{O}_7$  additives. On the other hand, their use resulted in the significant improvement of the ablation resistance, as the linear ablation rate of  $\text{ZrB}_2 - 25\text{vol. \% SiC}$  with 10 wt.% of  $\text{Yb}_2\text{O}_3$  and  $\text{Yb}_2\text{Zr}_2\text{O}_7$  was 3x lower when compared to the reference  $\text{ZrB}_2 - 25\text{vol. \% SiC}$ . No significant differences between the use of  $\text{Yb}_2\text{O}_3$  and  $\text{Yb}_2\text{Zr}_2\text{O}_7$  was observed, as a consequence of the fact that  $\text{Yb}_2\text{O}_3$  partially converted to  $\text{Yb}_2\text{Zr}_2\text{O}_7$  during the sintering.

### Acknowledgement



P.T. has received funding from the European Union's Horizon 2020 research and innovation programme under the Marie Skłodowska-Curie grant agreement No 798651. This work was supported by the Slovak Research and Development Agency under the contract no. APVV-17-0328 and APVV-SK-SRB-18-0022. The support of the Mobility project SAV-AVCR-21-04 is also acknowledged. This work was performed during the implementation of the project Building-up Centre for advanced materials application of the Slovak Academy of Sciences, ITMS project code 313021T081 supported by Research & Innovation Operational Programme funded by the ERDF.

## Design & development of precursor-derived ultra-high temperature resistant ceramic coatings and fibres for space applications

Ravi Kumar

Laboratory for High Performance Ceramics, Department of Metallurgical and Materials Engineering, Indian Institute of Technology-Madras (IIT Madras), Chennai 600036, India

Thermal barrier and environmental barrier coatings (TBCs and EBC's) are being extensively investigated and developed for the protection of metallic and Si-based ceramic components that are subjected to extremely harsh thermal environments. Rocket nozzle extension, guide vanes and combustor liners of spacecrafts are classic examples that require a specialized thermal/environmental protection owing to their prolonged exposure to hot corrosive environmental effects due to gas, moisture, debris including highly oxidizing atmospheres. The current state of art, zirconium and silicon-based TBC/EBCs are unable to withstand the severe thermo-oxidative environment, where the applicability and durability of coatings has become an important issue. Particularly, silicon material undergoes recession and hot corrosion mechanism of chemical degradation when exposed to water-containing high temperatures and alkali salts enriched environment resulting in the formation of volatile silicon hydroxide,  $\text{Si(OH)}_{4(g)}$  and alkali silicates.

Development of non-oxide, non-silicon based, rare earths-incorporated carbides and borides are of interest. Such ceramics have aroused greater attention since they are not only thermodynamically stable  $>2500\text{ }^\circ\text{C}$  but can also retard the inward transport/diffusion of oxygen. However, the *ex situ* addition of RE as a reinforcement results in several disadvantages such as poor homogeneity, adhesion and processing difficulties, which hinders widespread application. Our laboratory has been developing a new class of prime-reliant bond-coat-free Zr-RE-B-C ceramic coatings for Si-based composites (as EBCs) and for metallic alloys (as TBCs) for large-sized space components. In our recent research on Zr-La-B-C ceramic materials, it has been shown that nano-crystalline ultra-high temperature phases such as  $\text{ZrB}_2$ ,  $\text{ZrC}$ ,  $\text{LaB}_6$  and  $\text{La}_2\text{Zr}_2\text{O}_7$  can be in situ crystallized in a thermally stable amorphous matrix. Thermodynamic equilibrium phase calculations show that longer durations of heat-treatment may be required to achieve thermodynamic equilibrium. High-resolution transmission electron microscopy revealed encapsulation of nanocrystals ( $<5\text{ nm}$ ) in an amorphous matrix surrounded by turbostratic layers of carbon inhibiting its growth. Preliminary coating experiments have shown great promise (Figure-1). The laboratory has also been successful in producing ultra-high temperature ceramic fibres using an in-house developed centrifugal spinning set up and some of the promising preliminary results shall be shared.

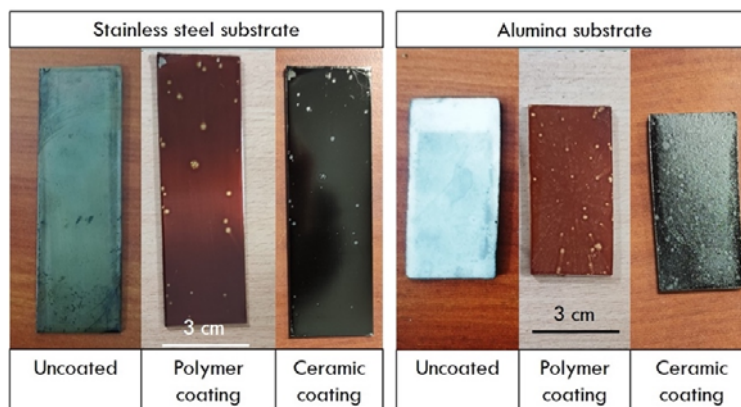


Figure-1 Coatings on metallic and ceramic substrates – figure shows both preceramic and pyrolyzed ceramic coatings

## Laser irradiation as an easy-to-apply method for Ti-based implant materials enhancement

**Ivana Cvijović-Alagić<sup>1</sup>, Sladana Laketić<sup>1</sup>, Miloš Momčilović<sup>1</sup>, Jovan Ciganović<sup>1</sup>, Đorđe Veljović<sup>2</sup>, Marko Rakin<sup>2</sup>**

<sup>1</sup>*Institute of Nuclear Sciences „Vinča“, University of Belgrade, P.O. Box 522, 11001 Belgrade, Serbia*

<sup>2</sup>*Faculty of Technology and Metallurgy, University of Belgrade, Karnegijeva 4, 11120 Belgrade, Serbia*

Hard-tissue replacements are most commonly made from the Ti-based materials, such as commercially pure titanium (CP-Ti) and Ti-6Al-4V (mass%) alloy, because of their exceptional biocompatible properties combined with the excellent corrosive and mechanical characteristics [1]. More recently, efforts have been made to additionally enhance the properties of the metallic implants through the careful selection of the alloy composition and surface modification technics [2,3]. As a result, second-generation  $\beta$ -type Ti alloys, containing non-toxic elements, have been developed. One of the promising  $\beta$ -type implant alloys is Ti-13Nb-13Zr (mass%). Even though the corrosion resistance and mechanical properties of this alloy are improved in comparison to the commonly used metallic implant materials, its biocompatible and osseointegration properties can and must be additionally enhanced. For that purpose several surface modification technics can be used, however, laser irradiation stands out as the most promising one. Because of that scope of the present research was to investigate the possibility of successful surface modification of the most commonly used implant material, *i.e.* CP-Ti, and the second-generation Ti-13Nb-13Zr alloy by utilizing the easy-to-apply laser irradiation method in order to obtain improved implant tribo-corrosive properties and enhanced biointegration and bioactivity.

Laser surface modifications were conducted using the Nd:YAG system in the air and argon atmosphere under different laser output energies. Implant materials surface morphologies after the laser irradiation treatment were investigated using the field-emission scanning electron microscopy (FE-SEM) and optical profilometry, while the impact of the laser irradiation on the implant materials surface characteristics were examined using the energy dispersive spectrometry (EDS) and microhardness measurements.

Conducted research showed that utilization of the Nd:YAG laser irradiation resulted in significant alterations of the CP-Ti and Ti-13Nb-13Zr alloy surface chemistry, morphology and microhardness. Laser irradiation of both investigated materials led to the formation of visible microcracks and hydrodynamic effects in the central part of the irradiated area, while traces of melted and solidified material were observed at its periphery. More pronounced morphological changes were induced during the laser irradiation in an argon atmosphere, while a higher degree of texturing was recorded at the surface of the Ti-13Nb-13Zr alloy. At the irradiated surfaces, the formation of the oxide layer, predominantly composed of Ti-oxide particles, was detected. Surface oxides are desirable since their presence can improve the implant material bioactivity with a simultaneous increase of the tribo-corrosive properties through the formation of the hard corrosion resistance surface film. Laser-induced chemical and morphological alterations were more distinctive in the case of the Ti-13Nb-13Zr alloy.

### References

- [1] M. Long, H.J. Rack, *Biomaterials*, 19 (1998) 1621.
- [2] M. Geetha, A.K. Singh, R. Asokamani, A.K. Gogia, *Prog. Mater. Sci.*, 54 (2009) 397.
- [3] X. Liu, P.K. Chu, C. Ding, *Mat. Sci. Eng. R*, 47 (2004) 49.

## **Innovative materials under extreme conditions: Multidisciplinary approach on multiscale level**

**Dejan Zagorac<sup>1,2</sup>**

*<sup>1</sup>Materials Science Laboratory, Institute of Nuclear Sciences “Vinča”, University of Belgrade, Belgrade, Serbia*

*<sup>2</sup>Center for synthesis, processing, and characterization of materials for application in the extreme conditions “CextremeLab”, Belgrade, Serbia*

Innovative materials used in high-technology applications are called advanced materials. High technology is the technology at the cutting edge, the most advanced technology available, bringing the most complex or the newest technology on the market, for example, computers (software and hardware), fiber-optic systems, space technology, aircraft, nuclear technology, etc. These materials can be typical traditional materials (e.g., metals, ceramics, polymers) whose properties have been enhanced or developed, to become advanced. This talk will cover theoretical investigation of various advanced materials with connection to the experimental results (e.g. oxides, sulfides, nitrides), especially under the influence of extreme pressure and temperature conditions. Furthermore, a plethora of the state-of-the-art quantum mechanical methods will be presented, including Density-functional theory (DFT), LDA-PZ and GGA-PBE, or hybrid B3LYP and HSE functionals, a combination of quantum mechanics with data mining and global optimization, as well as the newly developed PCAE method applied on ZnO/ZnS polytypic (hetero)structures and unknown (e.g. Cr<sub>2</sub>SiN<sub>4</sub>) compounds. Since many of the investigated materials show a large number of desirable properties for industrial applications, *ab initio* calculations of electronic, magnetic, elastic, and mechanical properties under extreme conditions will be presented and compared with experiments when available.

**INVITED LECTURES**  
**and**  
**ORAL PRESENTATIONS**

## Spinel-based ceramics for LEDs and photocatalytic applications

**Zoltán Lenčič, Mohamed Radwan, Patrícia Petrisková, Adriana Czimerová,  
Peter Boháč, Pavol Šajgalík**

*Institute of Inorganic Chemistry, Slovak Academy of Sciences, 84536 Bratislava, Slovakia*

Preparation and characterisation of transparent  $\text{MgAl}_2\text{O}_4$  and translucent  $\text{MgAlON}$  spinel ceramics doped with both transition and rare-earth metals will be presented. A systematic study was performed to develop a processing methodology for elimination of microstructural defects in sintered samples and improving the optical transparency. The powders were dispersed in a distilled water using Darvan C-N surfactant. Soft spinel granules with improved compressibility ( $I_c = 13$ ) were prepared by freeze granulation of stable suspensions in liquid nitrogen. Green compacts were prepared by CIP-ing under 400 MPa pressure. Spinel specimens with relative densities  $>99.9\%$  of theoretical were made by pressureless-sintering in air at 1550 °C and subsequent hot isostatic pressing at 1550 °C for 5 h in 200 MPa Ar gas. A similar process, but at 1800 °C was used for the preparation of  $\text{MgAlON}$  ceramics. The optical real in-line transmittance (RIT) of polished  $\text{MgAl}_2\text{O}_4$  specimens was 87% of the theoretical at the wavelength range of 425-705 nm.

A series of translucent spinel  $\text{MgAlON}$  phosphors doped with different cations were prepared. The colours of emissions depending on the dopant were as follows: Er – blue (451 nm), Eu – blue (460 nm), Ce – yellowish (570 nm) emission (Fig. 1). The chromium doped  $\text{MgAlON}$  phosphors excited by green light emitted dark-red light ( $\lambda_{em} = 715\text{-}720$  nm).

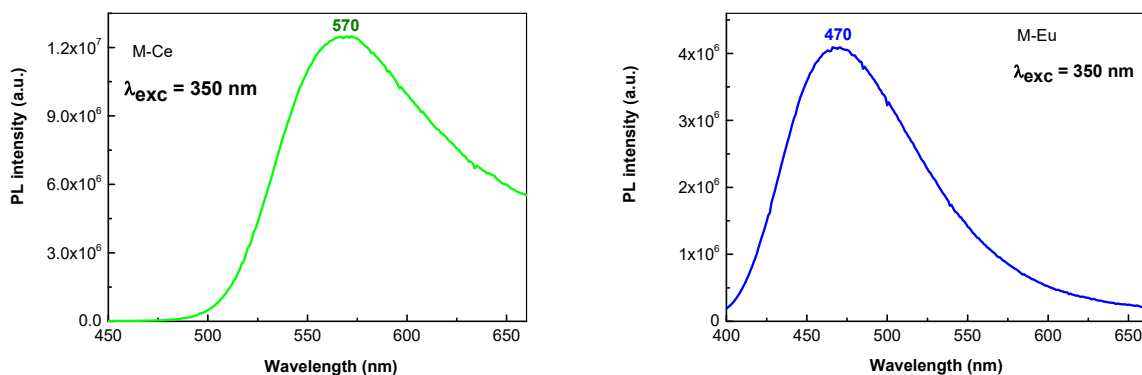


Fig. 1. Photoluminescence spectra of  $\text{MgAlON}:\text{Ce}$  and  $\text{MgAlON}:\text{Eu}$  phosphors.

Titania nanotubes were prepared by anodic oxidation of Ti layer deposited on transparent spinel ceramics. The transparent spinel ceramics combined with titania nanotubes will be tested for photocatalytic applications. The ceramic composites exhibited good removal/degradation of model pollutants: organic dye Rhodamine B and endocrine disruptor compound Bisphenol A.

### Acknowledgment

This work was supported by APVV-14-0385 and VEGA2/0164/18 projects. This work was performed during the implementation of the project Building-up Centre for advanced materials application of the Slovak Academy of Sciences, ITMS project code 313021T081 supported by Research & Innovation Operational Programme funded by the ERDF.



## Surface modification of Si<sub>3</sub>N<sub>4</sub> – Y<sub>2</sub>O<sub>3</sub> composites – optimisation of oxyacetylene torch conditions

Michal Hičák<sup>1</sup>, Miroslav Hnatko<sup>1,2</sup>, Zoltán Lenčész<sup>1</sup>, Pavol Šajgalík<sup>1</sup>

<sup>1</sup>*Institute of Inorganic Chemistry, Slovak Academy of Sciences, Dúbravská cesta 9, 845 36 Bratislava, Slovakia*

<sup>2</sup>*Centre of Excellence for Advanced Materials Application, Slovak Academy of Sciences, Dúbravská cesta 9, 84511, Bratislava, Slovakia*

Dense Si<sub>3</sub>N<sub>4</sub> substrates (98.2 % TD) with the addition of rare earths oxide (Y<sub>2</sub>O<sub>3</sub>) were prepared by rapid hot pressing at 1700 °C and 50 MPa pressure for 7 min. Yttria sintering additive was chosen because of the good oxidation resistance of Si<sub>3</sub>N<sub>4</sub>-Y<sub>2</sub>O<sub>3</sub> at elevated temperatures. Surface of the ceramic substrate was modified by oxyacetylene torch by means of formation of yttrium silicate based protective layer on the surface. The surface morphology and the character of damaged area was studied in dependence from the reached temperature on the surface of substrate, the dwell time on the annealing temperature, gas flow rate and the ratio of acetylene/oxygen gases. Finally, the influence of the mentioned parameters on the degree of oxidation of surface layer, its porosity, thickness and phase composition will be evaluated.

### Acknowledgment

This work was supported by the Slovak Research and Development Agency under the contract no. APVV-18-0542 and MVTS project of SAS “BioFun” within the scheme of JRP SAV-TUBITAK (No. 546676). This work was performed during the implementation of the project Building-up Centre for advanced materials application of the Slovak Academy of Sciences, ITMS project code 313021T081 supported by Research & Innovation Operational Programme funded by the ERDF.

## High Temperature Failures of Metals

**Gordana Bakic<sup>1</sup>, Milos Djukic<sup>1</sup>, Bratislav Rajcic<sup>2</sup>, Aleksandar Maslarevic<sup>2</sup>,  
Vesna Maksimovic<sup>3</sup>, Vladimir Pavkov<sup>3</sup>, Nenad Milosevic<sup>1</sup>**

<sup>1</sup> University of Belgrade, Fac. of Mechanical Engineering, , Kraljice Marije 16, Belgrade

<sup>2</sup> University of Belgrade, Innovation Center, Fac. of Mech. Eng., Kraljice Marije 16, Belgrade

<sup>3</sup> University of Belgrade, Vinca Institute of Nuclear Science, Vinca, Belgrade

Thermally activated processes and stresses lead to deterioration of mechanical and physical properties on the micro and macro level and damage over time when metals are used in the creep range. These deterioration processes in metals are temperature-, stress- and time- dependent [1,2]. Damage modes of metal alloys commonly used at high temperature could be divided into four main categories:

1. **Reduction of the cross section.** At very high temperatures (above  $0.8T_m$ ,  $T_m$  - melting temperature) the failure of pure metals and solid solutions most often occurs only due to extensive plastic deformation and the reduction of the cross section leading to the failure in final.

2. **Creep damage and weakening of the cross section.** Formation of pores within the grain or at the grain boundaries in perpendicular direction to maximum principal tensile stress causes weakening of the cross section leading to slow long term failure.

3. **Microstructural degradation.** Changes in the dislocation substructure and Increase in the dislocation density significantly affects the creep rate. When it comes to high stresses ( $\sigma = 0.5Re$ ), a cellular dislocation substructure is formed, which enables a higher rate of the recovery process and thus an increase in the creep rate. In addition, heat resistant alloys are precipitation hardened in their initial state with particles:  $\gamma'$ -particles in super alloys, carbides and nitrides in steels, etc. During long-term service at elevated temperature microstructural degradation, manifest itself in particle coarsening decreasing crack initiation and crack growth resistance.

4. **Interaction with the environment.** Damage caused by internal oxidation is a consequence of the penetration of oxygen into the metal, except when it participates in the formation of a protective oxide layer. Oxygen diffusing into the metal reacts with the impurities, creating an internal oxidation zone, Fig. 1. Extensive surface oxidation lead to disturbance in heat transfer and changes in metal wall temperature consequently often accelerating creep processes (overheating). During dynamic loading oxidation could lead to and local damage of the thermal fatigue type.

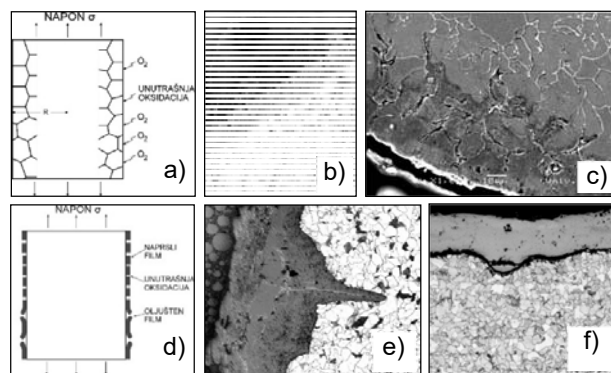


Figure 1. Oxidation [2]: a) schematic representation of internal oxidation of: b) austenitic steel and c) low-alloy steel); e) schematic representation of external oxidation: e) on the gas side and f) on the steam side

### References

[1] G. Bakic, M. Djukic, Vera Sijacki Zeravcic: Basic Failure Mechanisms of Engineering Structures, Fac. of Mech Engineering, Belgrade, 2021.

[2] Н.В.Бугай, Березина Т.Г., Трунин И.И., Работоспособность и долговечность металла энергетического оборудования, Энергоатомиздат, Москва, 1994.

## Hydrogen embrittlement mechanisms in steels at different length scales

Milos B. Djukic<sup>1</sup>, Gordana M. Bakic<sup>1</sup>, Vera Sijacki Zeravcic<sup>1</sup>, Bratislav Rajjicic<sup>1</sup>,  
Aleksandar Sedmak<sup>1</sup>, Muhammad Wasim<sup>2</sup>, Jovana Perisic<sup>1</sup>

<sup>1</sup> University of Belgrade, Faculty of Mechanical Engineering,  
Kraljice Marije 16, 11120 Belgrade 35, Serbia

<sup>2</sup> School of Engineering, Infrastructure Department, The University of Melbourne,  
3010 Parkville, Melbourne Australia

Component failures due to the hydrogen embrittlement (HE) were observed in different industrial systems, including high-pressure hydrogen storage tanks, aircraft components, high-strength alloy components, and high-strength steel fasteners [1,2]. The contemporary approach in studying the effects of hydrogen on the mechanical properties of steels at different scales is based on the implementation of various multiscale (macro, micro-meso, and nano-atomic) modeling approaches and the applications of advanced multiscale experimental methods, Fig. 1 [3]. Simultaneous action in a cooperative manner of the hydrogen-enhanced localized plasticity (HELP) and the hydrogen-enhanced decohesion (HEDE) mechanism of HE, according to the HELP + HEDE model [4] of HE, were confirmed to be active, depending on the local concentration of hydrogen in steel [2-5], Table 1 [2]. Further investigations of the mechanical properties of steels at different length scales exposed to hydrogen damage should open a new window in the research related to the simultaneous action of HE mechanisms. It will also provide improved maintenance and the accurate service life prediction of various industrial components exposed to multiple active HE mechanisms [5,6].

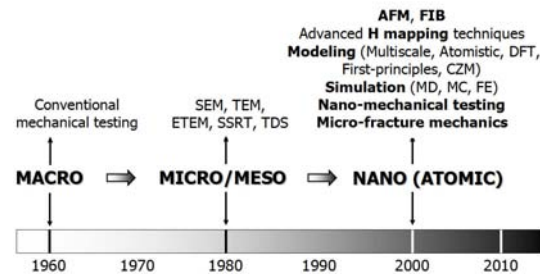


Fig. 1. Historical overview and shift in HE study approaches (macro → micro-meso → nano-atomic) [3].

Table 1. Summary of active HE mechanisms in low carbon steel, grade 20 (St.20 or 20G, equivalent to AISI 1020) [2].

Charpy specimen	Distance (mm)	Hardness (HV5)	KCV <sub>TOT</sub> (J/cm <sup>2</sup> )	KCV <sub>P</sub> (J/cm <sup>2</sup> )	KCV <sub>I</sub> (J/cm <sup>2</sup> )	Fracture modes	Active hydrogen embrittlement (HE) / damage mechanisms
S2	3	156	40.74	29.86	10.88	MVC + TG	HELP
S6	6	166	36.07	25.13	10.84	MVC + TG (MVC >> TG)	HELP + HEDE model [4] HELP > HEDE
S5	3	167	17.13	8.40	8.70	TG + MVC (TG >> MVC)	HELP + HEDE model [4] HEDE > HELP → sharp DBT
S4	-	183	9.84	2.98	6.83	TG + IG, voids	HEDE + HTHA

### References

- [1] Popov, B.N., Lee, J.W., Djukic, M.B. Hydrogen permeation and hydrogen-induced cracking, In: Handbook of Environmental Degradation of Materials, Third Edition, William Andrew Publishing, 2018, pp. 133-162. <https://doi.org/10.1016/B978-0-323-52472-8.00007-1>
- [2] Djukic, M.B., Bakic, G.M., Sijacki Zeravcic, V., Sedmak, A., Rajjicic, B. Hydrogen embrittlement of industrial components: prediction, prevention, and models, *Corrosion* 2016;72(7): 943-961. <https://doi.org/10.5006/1958#>
- [3] Djukic, M.B., Bakic, G.M., Sijacki Zeravcic, V., Sedmak, A., Rajjicic, B. The synergistic action and interplay of hydrogen embrittlement mechanisms in steels and iron: Localized plasticity and decohesion, *Eng. Fract. Mech.* 2019;216:106528. <https://doi.org/10.1016/j.engfracmech.2019.106528>
- [4] Djukic, M.B., Sijacki Zeravcic, V., Bakic, G.M., Sedmak, A., Rajjicic, B. Hydrogen damage of steels: a case study and hydrogen embrittlement model, *Eng. Fail. Anal.* 2015;58: 485-498. <https://doi.org/10.1016/j.engfailanal.2015.05.017>
- [5] Wasim, M., Djukic, M.B. Hydrogen embrittlement of low carbon structural steel at macro-, micro- and nano-levels, *Int. J. Hydrogen Energ.* 2020;45(3):2145-2156. <https://doi.org/10.1016/j.ijhydene.2019.11.070#>
- [6] Wasim, M., Djukic, M.B., Ngo, T.D. Influence of hydrogen-enhanced plasticity and decohesion mechanisms of hydrogen embrittlement on the fracture resistance of steel, *Eng. Fail. Anal.* 2021;123: 105312. <https://doi.org/10.1016/j.engfailanal.2021.105312#>

## Silicon carbide - graphene composites with high functional properties

**Ondrej Hanzel<sup>1</sup>, Zoltán Lenčes<sup>1</sup>, Young-Wook Kim<sup>2</sup>, Ján Fedor<sup>3</sup>, Pavol Šajgalík<sup>1</sup>**

<sup>1</sup>*Institute of Inorganic Chemistry, Slovak Academy of Sciences, Dúbravská cesta 9, 845 36 Bratislava, Slovak Republic*

<sup>2</sup>*Functional Ceramics Laboratory, Department of Materials Science and Engineering, University of Seoul, Seoul 02504, Republic of Korea*

<sup>3</sup>*Institute of Electrical Engineering, Slovak Academy of Sciences, Dúbravská cesta 9, 845 36 Bratislava, Slovak Republic*

Dense silicon carbide/graphene nanoplatelets and silicon carbide/graphene oxide composites with 1 vol.% equimolar  $Y_2O_3$ – $Sc_2O_3$  sintering additives were sintered by rapid hot pressing technique at 2000°C in nitrogen atmosphere. As sintered composites were annealed in gas pressure sintering (GPS) furnace at 1800°C for 6 h in the overpressure of nitrogen (3 MPa). Effects of graphene plates orientation, type and amount of graphene as well as the influence of annealing conditions on the thermal and electrical properties and microstructure of prepared composites were investigated. The electrical conductivity of reference SiC sample ( $17 \text{ S}\cdot\text{cm}^{-1}$ ) gradually increased with increasing GO or GNP content, reaching the highest value of  $67 \text{ S}\cdot\text{cm}^{-1}$  for SiC with 10 wt.% GNPs. Remarkable improvement of electrical conductivity was achieved by annealing the samples in  $N_2$  atmosphere and the highest value of  $118 \text{ S}\cdot\text{cm}^{-1}$  was obtained for the sample with 10 wt.% GNPs. The highest thermal conductivities were obtained at room temperature in parallel direction to GNPs for annealed SiC samples with 1% GO ( $\lambda = 238 \text{ W}\cdot\text{m}^{-1}\cdot\text{K}^{-1}$ ) and 5% GNPs ( $\lambda = 233 \text{ W}\cdot\text{m}^{-1}\cdot\text{K}^{-1}$ ). The obtained results show that appropriate choice of sintering additives, application of freeze granulation, rapid hot-pressing and annealing of samples at 1800 °C for 6h in  $N_2$  atmosphere allows to obtain SiC ceramics with very high electrical and thermal conductivity.

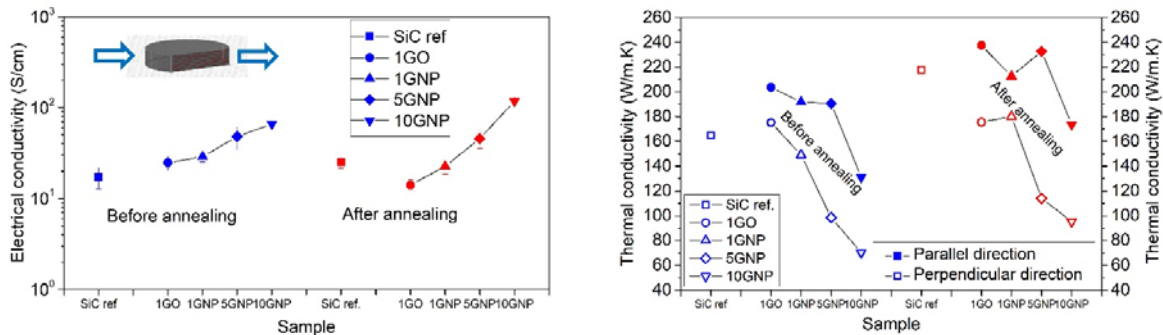


Fig. 1: Electrical and thermal conductivity of SiC-GNPs and SiC-GO composites in direction parallel and perpendicular to graphene layers.

### Acknowledgements

This work was performed during the implementation of the project Building-up Centre for advanced materials application of the Slovak Academy of Sciences, ITMS project code 313021T081 supported by Research & Innovation Operational Programme funded by the ERDF. This work was also supported by the Slovak grant VEGA 2/0007/21.

## Preparation and characterization of B<sub>4</sub>C/TiB<sub>2</sub> composites

**Hakan Ünsal<sup>1</sup>, Ondrej Hanzel<sup>1</sup>, Salvatore Grasso<sup>2</sup>, Alexandra Kovalčíková<sup>3</sup>, Ivo Dlouhý<sup>4</sup>,  
Peter Tatarko<sup>1\*</sup>**

<sup>1</sup>*Institute of Inorganic Chemistry, Slovak Academy of Sciences, Dubravská cesta 9, 845 36,  
Bratislava, Slovakia*

<sup>2</sup>*Key Laboratory of Advanced Technologies of Materials, Ministry of Education, School of  
Materials Science and Engineering, Southwest Jiaotong University, Chengdu, 610031, China*

<sup>3</sup>*Institute of Materials Research, Slovak Academy of Sciences, Watsonova 47, 040 01 Kosice,  
Slovakia*

<sup>4</sup>*Institute of Physics of Materials, Czech Academy of Sciences, Žitkova 22, 616 00, Brno, Czech  
Republic*

In this study, the boron carbide matrix composites were fabricated using a Field Assisted Sintering Technology (FAST). The composites containing 10 vol% TiB<sub>2</sub> particles were prepared by in situ reaction of B<sub>4</sub>C, TiO<sub>2</sub> powder and carbon black. The effect of different processing parameters, such as degassing step, and sintering time, on the sintering behaviour of B<sub>4</sub>C was studied in the temperature range of 1800 °C to 2000 °C and the pressure of 70 MPa.

The microstructures of the B<sub>4</sub>C/TiB<sub>2</sub> composites were characterized by X-Ray Diffraction, Scanning Electron Microscope and Raman Spectroscopy. The results showed that homogeneous microstructure and fully dense B<sub>4</sub>C-10vol.%TiB<sub>2</sub> materials were obtained using the sintering regime with a degassing step at the temperature of 1800 °C, followed up by the applying of maximum pressure for 30s. Interestingly, when the critical sintering conditions were exceeded, the in-situ formation of graphene platelets in the middle part of the materials was observed. Due to the low electrical resistance of TiB<sub>2</sub> at high temperatures, the TiB<sub>2</sub> grains provided a pathway for electric current. This caused the local overheating at the grain boundaries between B<sub>4</sub>C and TiB<sub>2</sub>, which led to the local decomposition of B<sub>4</sub>C and in-situ formation of graphene platelets. This problem was prevented by changing the direction of electric current. The mechanical properties of B<sub>4</sub>C, such as hardness, strength and fracture toughness, were improved by the addition of in-situ formed TiB<sub>2</sub> particles.

### Acknowledgement

This work was supported by the Slovak Research and Development Agency under the contract no. APVV-17-0328 and APVV-SK-SRB-0022. The support of the Mobility project SAV-AVCR-21-04 is also acknowledged. This work was performed during the implementation of the project Building-up Centre for advanced materials application of the Slovak Academy of Sciences, ITMS project code 313021T081 supported by Research & Innovation Operational Programme funded by the ERDF.

## Luminescence properties of Eu<sup>3+</sup>-doped Mayenite under high pressure

**Branko Matovic<sup>1</sup>, Marija Prekajski Djordjevic, Marko Nikolic<sup>2</sup>**

<sup>1</sup>University of Belgrade, Vinca Institute of Nuclear Sciences

<sup>2</sup>University of Belgrade, Institute of Physics

Europium doped mayenite (C12A7) powders of different concentration (0.5, 1.0, 1.5 and 2.0 at.%) have been synthesized by modified glycine/nitrate procedure - MGNP). Obtained samples were characterized by X-ray diffraction (XRD), field emission scanning electron microscopy (FE-SEM), and steady state photoluminescence spectroscopy. The photoluminescence spectra measurements were done under continuous Nd YAG laser excitation at 532 nm. Data were collected from Ocean Optics USB2000 (200-800 nm) spectrometer. High-pressure luminescence was measured in a Betsa high pressure membrane diamond anvil cell up to 23 GPa with steel gasket (T301). Sample chamber was 125  $\mu\text{m}$  in diameter and 70  $\mu\text{m}$  in thickness. A mixture of methanol and ethanol with a 4:1 volume ratio was selected as the pressure-transmitting medium. Ruby loaded with sample determine the pressure. For measuring Ruby R1 line shift HR2000 Ocean Optics spectrometer (600-800 nm) was used. The effect of doping concentration on photoluminescence properties of Eu<sup>3+</sup> doped mayenite were studied and are discussed. With the increasing of Eu<sup>3+</sup> doping concentration, the red emitting intensity exhibited a behavior that increased firstly and then decreased. The optimal Eu<sup>3+</sup> ion concentration is found to be 1.5%. Obtained results suggest that C12A7: Eu phosphor may serve as a promising red luminescent materials used in fabrication of optical storage and illumination in dark environments.

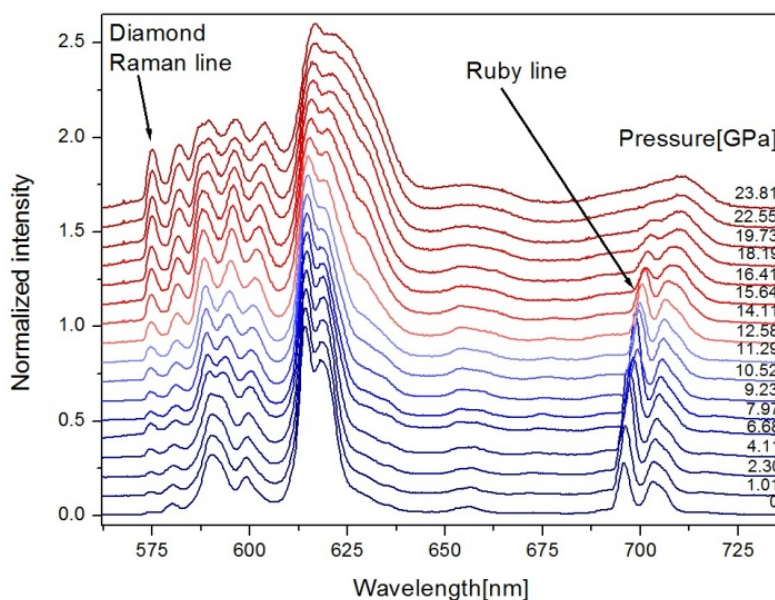


Figure 1. Pressure dependence of Emission spectrum Eu<sup>3+</sup>-doped Mayenite.

### References

[1] B Matović, M Prekajski, J Pantić, T Bräuniger, M Rosić, D Zagorac, B. Babic, Synthesis and densification of single-phase mayenite (C12A7), *Journal of the European Ceramic Society* **36** (2016) 4237-4241.

## Development of Highly Microstructure-Controlled Alumina Ceramics

**Jelena Maletaškić<sup>1</sup>, Joshua Emory<sup>2</sup>, Anna Gubarevich<sup>3</sup>, Liao Nengqing<sup>3</sup>, Katsumi Yoshida<sup>3</sup>**

<sup>1</sup>*Centre of Excellence-CextremeLab, Vinča Institute of Nuclear Sciences, University of Belgrade, Belgrade, Serbia*

<sup>2</sup>*Laboratory for Advanced Nuclear Energy, Institute of Innovative Research, Tokyo Institute of Technology, Tokyo, Japan*

<sup>3</sup>*University of Wisconsin – Madison, Department of Materials Science and Engineering, Wisconsin, USA*

Alumina ceramics that resembles seashells are made of aligned micron-sized monocrystalline platelets joined together by silica secondary phase. Due to its high hardness, high melting point, high refractory index, these composites provides an attractive combination of ease of processing, high strength, and high toughness. Sea shells consist mostly of platelets  $\text{CaCO}_3$ , with a small amount of a biopolymer ( 1 – 5 %). This forms a layered structure like a brick wall, that gives rise to high bending strength and fracture toughness. By using alumina with a plate like crystal structure, to mimics the  $\text{CaCO}_3$ , and  $\text{SiO}_2$  as a to mimic the biopolymer, the microstructure can be made to look like and act like that of a sea shell. Dense alumina – silica samples were syntesied using hot press sintering at  $1500^\circ\text{C}$ . Samples of particle size  $2.0\mu\text{m}$  resulted in maximum strength and improved hardness  $2.0\mu\text{m}$  plate resembled the microstructure of sea shell the most.

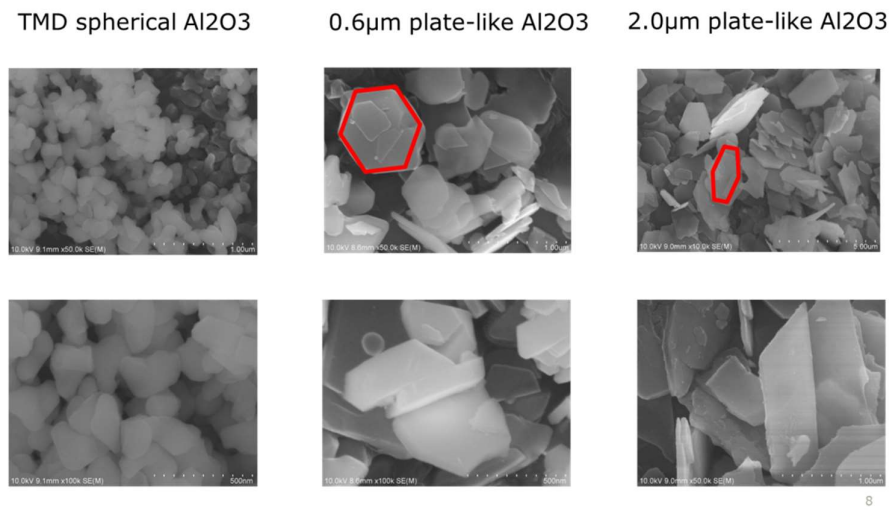


Figure 1. SEM micrographs of used alumina powders.

## Electrodeposition of powders in vigorous hydrogen evolution conditions

**Vesna Maksimović<sup>1</sup>, Nebojša Nikolić<sup>2</sup>**

<sup>1</sup>Department of Materials Science, CEXTREME LAB, Institute of Nuclear Sciences “Vinča”,  
University of Belgrade, Mike Petrovića Alasa 12-14, 11000 Belgrade, Serbia

<sup>2</sup>ICTM-Department of Electrochemistry, University of Belgrade, Njegoševa 12, P. O. Box 473,  
11001 Belgrade, Serbia

Electrolysis is one of the most commonly used method for synthesis of metals and alloys in the powder form. The advantages of this method in relation to the other methods, such as atomization processes, melt spinning, rotating electrode process (REP), mechanical and chemical processes, are: low equipment and product costs, one-step and environmentally friendly process, formation of high purity products, *etc.* The electrolytically produced powders are highly pure and can be easily sintered and pressed. These powders belong to the group of disperse or irregular deposits which spontaneously fall from the electrode surface or are removed from it by tapping or on some similar way. Various powdered forms can be obtained by electrolysis: dendrites, wires or needles, spongy-like, flakes, fibrous and cauliflower-like forms. The shape and size of produced particles depend on the conditions and regimes of electrolysis, the presence of additive, hydrogen evolution as a parallel reaction, and the nature of metals.

The processes of electrolysis in the hydrogen co-deposition range represent an important segment in investigation of powder formation, and these processes are a feature of metals characterized by medium and low values of both the exchange current density and overpotential for hydrogen discharge. Metals with these characteristics are denoted as either *intermediate* (Cu) or *inert* (Ni, Co, Fe, Pt, Pd) metals. One of the main benefits of the usage of electrodeposition processes with parallel hydrogen evolution is the possibility of formation deposits with very high surface area and nanostructural characteristics, such as the honeycomb-like or the 3D (three-dimensional) foam structures. The main characteristic of these deposits is the presence of holes or pores formed by the detachment of hydrogen bubbles surrounded by cauliflower-like or dendritic particles. Almost all metals from the groups of *intermediate* and *inert* ones are formed in the honeycomb-like or the 3D foam forms, e.g. Cu [1] and Co [2]. Aside from pure metals, some alloys like Ni-Co can be deposited in this form [3].

The Fig. 1(a,b) shows morphologies of metal (Co) and alloy (Ni-Co) powder particles electrodeposited in vigorous hydrogen evolution conditions.

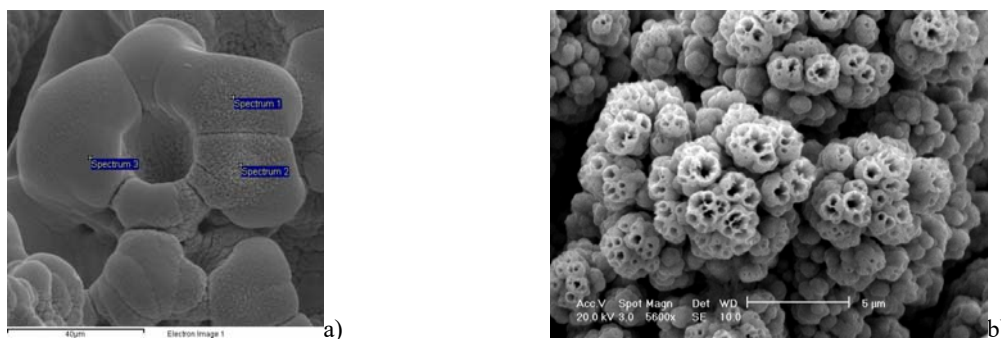


Figure 1. Morphology of (a) spongy-like Co powder particles obtained by electrodeposition at a current density of 770 mA cm<sup>-2</sup> and (b) Ni-Co powder particles obtained at a current density of 100 mA cm<sup>-2</sup>.

### References

- [1] K.I. Popov, S.S. Djokić, N.D. Nikolić, V.D. Jović, Morphology of Electrochemically and Chemically Deposited Metals, Springer: New York, USA, 2016, pp. 1–368.
- [2] V.M. Maksimović, N.D. Nikolić, V.B. Kusigerski, J.L. Blanuša, J Serb Chem Soc, 80 (2015) 197.
- [3] V.M. Maksimović, V.B. Kusigerski, M.M. Stoiljković, J.R. Maletaškić, N.D. Nikolić, T Nonferr Metal Soc, 30(4) (2020) 1046



## Supercritical Hydrothermal Synthesis of ceramic powders in batch conditions

**Marjan Randelović<sup>1</sup>, Aleksandra Zarubica<sup>1</sup>, Branko Matović<sup>2</sup>**

<sup>1</sup>*Faculty of Science and Mathematics, University of Niš, 18000 Niš, Serbia*

<sup>2</sup>*”Vinča” Institute of Nuclear Sciences, University of Belgrade, 11000 Belgrade, Serbia*

The water under supercritical conditions is an excellent reaction medium for crystallization of metal oxide particles due to the drastic change water characteristics around the critical point: density, dielectric constant and ionic product. Therefore, this approach is considered as a green solvent process suitable for the synthesis of different simple and complex oxides.

The first part of this study concerns the mechanism of the reactions, outstanding features of the supercritical water, the batch-type reactor synthesis and applications. The second part of the study describes the batch reaction process as a useful technique for the synthesis of bare and doped CeO<sub>2</sub> under supercritical hydrothermal conditions. Ceramic powders synthesized by this method usually have superior properties than the powders obtained by conventional high-temperature synthesis. Additionally, synthesis in supercritical water reduces energy consumption and the alkaline concentration for the production of highly crystalline and size-controlled metal oxide particles. The reaction rate for the synthesis of multi metal oxide compounds is enhanced more than 10<sup>3</sup> times under the supercritical conditions than under the conventional hydrothermal conditions due to the low dielectric constant (<10) ensuring the products with high crystallinity.

Processing of ceramic materials under supercritical hydrothermal conditions is a promising technique which could be transferred from laboratory scale to industry and potentially boost economic growth and promote environmental sustainability.

### References

- [1] T. Adschiri, Y. Hakuta, K. Arai, Hydrothermal Synthesis of Metal Oxide Fine Particles at Supercritical Conditions, *Ind. Eng. Chem. Res.* 39, 12, (2000) 4901-4907
- [2] A. Yoko, T. Aida, N. Aoki, D. Hojo, M. Koshimizu, S. Ohara, G. Seong, S. Takami, T. Togashi, T. Tomai, T. Tsukada, T. Adschiri, Application 53 - Supercritical Hydrothermal Synthesis of Nanoparticles, *Nanoparticle Technology Handbook* (Third Edition), 2018, Pages 683-689
- [3] H. Hayashi, Y. Hakuta, Hydrothermal Synthesis of Metal Oxide Nanoparticles in Supercritical Water, *Materials*. 3 (2010) 3794-3817

## Layer formation on ternary Ni-10Cr-1Si (in wt.%) alloy upon low temperature gaseous nitriding

**Matej Fonović<sup>1</sup>, Lovro Liverić<sup>1</sup>, Neven Tomašić<sup>1</sup>, Zoran Knežević<sup>2</sup>**

<sup>1</sup>University of Rijeka, Faculty of Engineering, Vukovarska 58, 51000 Rijeka, Croatia

<sup>2</sup>Electroindustrial and trade school Rijeka, Zvonimirova 12, 51000, Rijeka, Croatia

Gaseous nitriding is very important thermochemical surface treatment which involves the diffusion of nitrogen into the surface-adjacent area of various metals and alloys. For some materials this can be a desired process leading to improved mechanical and chemical properties of the treated material, e.g. in iron, steel and Ni-based alloys [1]. The nitriding behaviour and layer formation on ternary Ni-10Cr-1Si (in wt.%) alloy has now been studied in ammonia and hydrogen gas mixture over the range of 300-500 °C for 5, 15 and 40 hours. The microstructure of the above mentioned

alloy nitrided at 300 °C shows formation of a very thin surface layer accompanied with thicker diffusion zone (cf. Figure 1). Phase analysis performed by XRD shows presence of Ni<sub>3</sub>N in a form of compound layer, CrN precipitates, and so-called expanded austenite phase ( $\gamma_N$ ) (cf. Figure 2). Furthermore, the existence of silicon nitride was not confirmed by any of the techniques and methods used in this study. The expanded austenite Bragg reflection observed by XRD shows: (i) asymmetric dependent broadening of the corresponding Bragg reflections which depends on the nitrogen concentration gradient, and (ii) obvious *hkl* shift of the expanded austenite Bragg reflection as a consequence of composition induced macrostress, similarly as reported in Ref [2]. The nitrogen depth-concentration profile obtained from the measurements on a sample cross-section indicates that the nitrogen concentration decreases monotonously with increasing depth. As a result of the nitriding treatment surface hardness increases several times where all microstructural constituents ( $\gamma_N$ , CrN and Ni<sub>3</sub>N) contribute to the increased hardness of the nitrided zone. When comparing nitriding parameters (temperature, time and nitriding potential) increase in treatment temperature produces higher surface hardness than the increase of the nitriding potential and/or duration of the treatment. Occasionally cracks are observed in the sample morphology as a consequence of very high internal residual stresses developed upon nitriding treatment.

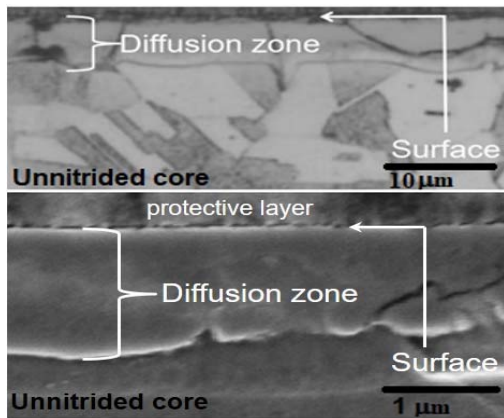


Figure 1. Light-optical and SEM micrograph showing typical microstructure developed upon nitriding of ternary Ni-10Cr-1Si alloy.

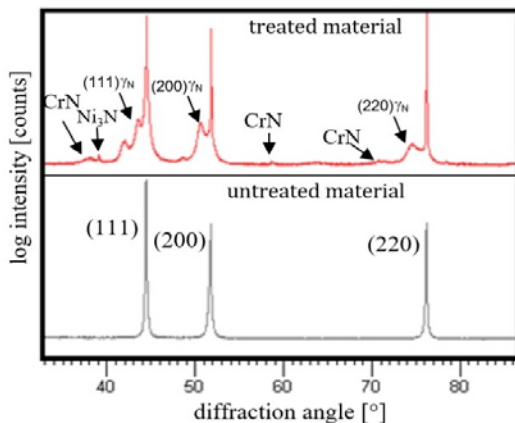


Figure 2. The XRD patterns obtained from the unnitrided and of the nitrided Ni-10Cr-1Si alloy indicating different microstructural constituents.

### References

- [1] F. Borgioli, *Metals*, 10(2) (2020) p. 187
- [2] M. Fonović, A. Leineweber, O. Robach, E.A. Jägler, and E.J. Mittemeijer, *Metall. Mater. Trans. A*, 46 (2015) pp. 4115

## Predicting stable modifications of Ce<sub>2</sub>ON<sub>2</sub> using a combination of global optimization and data mining

Jelena Zagorac<sup>1,2</sup>, Christian J. Schön<sup>3</sup>, Dušica Jovanović<sup>1,4</sup>, Dejan Zagorac<sup>1,2</sup>, Tamara Škundrić<sup>1,4</sup>, Milan Pejić<sup>1,5</sup>, Branko Matović<sup>1,2</sup>

<sup>1</sup>Materials Science Laboratory, Institute of Nuclear Sciences “Vinča”, University of Belgrade, Belgrade, Serbia

<sup>2</sup>Center for synthesis, processing, and characterization of materials for application in the extreme conditions “CextremeLab”, Belgrade, Serbia

<sup>3</sup>Max Planck Institute for Solid State Research, Heisenbergstr. 1, 70569 Stuttgart, Germany

<sup>4</sup>Department of chemistry, Faculty of science and mathematics, University of Nis, Nis, Serbia

<sup>5</sup>Faculty of Physics, University of Belgrade, Belgrade, Serbia

In this study the energy landscape of the hypothetical ionic cerium oxynitride Ce<sub>2</sub>ON<sub>2</sub> ceramic has been explored [1]. As the result we have predicted several stable modifications for this compound for the first time. The discovery of new modifications in the predicted system has been achieved using global optimization and data mining, where the energy landscape has been explored for various pressures and different numbers of formula units in the simulation cell. Each structure optimization has been performed with empirical potentials and on the *ab initio* level, in order to get higher accuracy of the results. From more than 14000 structure candidates obtained after global optimization with simulated annealing and starting with 29 potential structures after performing the data mining and prototyping, we have obtained five highly plausible low-energy modifications that could be realized as (meta)stable modifications, plus seven crystallographically and chemically interesting but energetically unfavorable structures.

The  $\alpha$ -Ce<sub>2</sub>ON<sub>2</sub> modification, with an AlCo<sub>2</sub>Pr<sub>2</sub>-like structure, is predicted to be the thermodynamically stable modification at standard conditions, while at effective negative pressures, the  $\beta$ -Ce<sub>2</sub>ON<sub>2</sub> modification should be thermodynamically stable and synthetically accessible. Two predicted orthorhombic modifications might be stable at high temperatures, the already mentioned  $\beta$ -modification and the  $\gamma$ -modification. Finally, high temperatures combined with high pressures might favor the  $\delta$ - or the  $\epsilon$ -modification, two closely related structures. Clearly, this is only a first step towards the full phase diagram in the Ce-O-N system. Nevertheless, this work provides a first glimpse of the potential structural richness of the Ce-O-N system, and supports attempts to synthesize the predicted modifications of Ce<sub>2</sub>ON<sub>2</sub>, guided by our analysis of the energy landscape of this chemical system.

### References

[1] J. Zagorac, J.C. Schön, B. Matović, T. Škundrić, D. Zagorac, Predicting Feasible Modifications of Ce<sub>2</sub>ON<sub>2</sub> Using a Combination of Global Optimization and Data Mining, Journal of Phase Equilibria and Diffusion, 41 (2020) 538-549.

## Generation of a Laser-Supported Detonation (LSD) Wave

**Milovan Stoiljković, Suzana Veličković, Filip Veljković, Đorđe Kapuran**

*University of Belgrade, VINČA Institute of Nuclear Sciences-National Institute of the Republic of Serbia, Department of Physical Chemistry, Mike Petrovića Alasa 12-14, 11000, Belgrade, Serbia*

When a focused laser beam reaches a certain threshold power density, a gas breakdown may take place. The laser-induced plasma (LIP) occurs due to optical breakdown and, consequently, a shock wave arises reaching over hypersonic speeds. In this case, the initiated plasma propagates backward of the target but also produces a shock wave that also propagates backward, as well as sideways. To explain this effect, a mechanism of a radiation-supported shock wave or, laser-supported detonation (LSD) wave was proposed.

Here we report the spectroscopic diagnostic of LIP generated in an argon atmosphere water aerosol and dynamics of aroused LSD wave by measuring the Stark width and Doppler redshift of the H $\alpha$  656.28 nm line. The hydrogen originates from the water dissociation from the aerosol.

A Transversely Excited Atmospheric (TEA) CO $_2$  laser was applied for plasma generation. TEA laser emits at 10.6  $\mu\text{m}$  furnishing typically 140 mJ of output energy in  $\sim 2$   $\mu\text{s}$  pulse duration and repetition rate 1-2 Hz [1]. The entire pulse can be considered as two consecutive pulses. The first pulse lasts 100 ns (gain-switched spike) and the second lasts  $\sim 1100$  ns. The focus area is typically 1.5 mm $^2$  giving the resulting peak fluencies of 310 kW mm $^{-2}$  and 55 kW mm $^{-2}$ . The laser is focused on the tantalum interface. Alongside the interface, a flow of water aerosol was generated through a Meinhard-type pneumatic nebulizer. The supporting gas is argon and the resulting aerosol contains 0.04 H $_2$ O per Ar (mole ratio). After striking the interface, the resulting LIP expands sideways and backward, i.e. toward the incident laser beam, and penetrates the aerosol. The plasma plume was scanned laterally to obtain space-resolved plasma parameters.

The measured H $\alpha$  Stark widths range 0.5-1.3 nm giving the LIP electron density range 1-3.5 $\cdot 10^{23}$  m $^{-3}$  which is in agreement with a computer-simulated calculus for atmospheric two-component plasma (H and Ar $^+$ ) in a temperature range 5-10 $\cdot 10^3$  K and perturbed mass of 0.9 [2]. The H $\alpha$  line redshifts starts at a 3.5 mm distance from the interface which corresponds to a time of 0.7  $\mu\text{s}$  of the full pulse duration. Starting that distance, a powerful LSD wave develops with an initial acceleration of about 1500 kms $^{-2}$  reaching a maximum velocity of 24 kms $^{-1}$  at a distance of 5.5 mm. The LSD wave dynamic is very well approximated by the Sedov-Tyler model. According to that model, the LSD wave propagation geometry here is spherical and the shock wave carries about 40% of the input laser energy ( $\sim 60$ mJ) [3]. Taking that the shock wave was registered over 0.2  $\mu\text{s}$  its resulting power is about 30 kW.

### References

- [1] Jelena Savović, Milovan Stoiljković, Miroslav Kuzmanović, Miloš Momčilović, Jovan Ciganović, Dragan Ranković, Sanja Živković, Milan Trtica, Spectrochim Acta Part B, 118 (2016) 127
- [2] M. Gigosos, M. Gonzalez, V. Cardenoso, Spectrochim Acta Part B, 58 (8) (2003) 1489
- [3] Koichi. Mori, Kimiya. Komurasaki, J. of Appl. Phys., 95 (11) (2004) 5979

## The Effects of Swift Heavy Ion Irradiation on Structural Properties of Glassy Carbon

**Zoran Jovanović<sup>1</sup>, Andrzej Olejniczak<sup>2</sup>, Nina Daneu<sup>3</sup>, Matjaž Spreitzer<sup>3</sup>, Danica Bajuk-Bogdanović<sup>4</sup>, Željko Mravik<sup>1</sup>, Vladimir Skuratov<sup>2</sup>**

<sup>1</sup> Center of Excellence for Hydrogen and Renewable Energy, Laboratory of Physics, Vinča Institute of Nuclear Sciences, University of Belgrade, P.O. Box 522, Belgrade, Serbia

<sup>2</sup> Flerov Laboratory of Nuclear Reactions, Joint Institute for Nuclear Research, 141980 Dubna, Russia

<sup>3</sup> Advanced Materials Department, Jožef Stefan Institute, 1000 Ljubljana, Slovenia

<sup>4</sup> Faculty of Physical Chemistry, University of Belgrade, P.O. Box 47, Belgrade, Serbia

When placed in extreme environments, materials can behave in unexpected and unpredictable ways. Thus, understanding the material behavior in such cases is critical to designing new advanced materials and assuring their safety and reliability.

In the present study the effects of swift heavy ion irradiation (167 MeV Xe<sup>26+</sup>,  $6 \times 10^{11} - 1 \times 10^{14}$  ions cm<sup>-2</sup>) on the structural properties of glassy carbon have been examined by using Raman spectroscopy, X-ray diffraction (XRD) and transmission electron microscopy (TEM). XRD analysis has shown an increase of disorder in irradiated samples *i.e.* reduced crystallinity and increased interlayer spacing. More precise structural information was obtained by analyzing the cross-section of the samples. TEM analysis identified four regions whose total thickness is matching the penetration depth predicted by SRIM. Besides region of reduced crystallinity, the TEM analysis revealed that topmost layer (~320 nm) is being amorphized. Raman analysis revealed regions in which structural degradation is either dominated by electronic or nuclear losses. Moreover, it helped to identify a region in which *sp*-carbons chains are being formed due to interaction with ions.

The obtained results improve the understanding of structural changes appearing in glassy carbon upon swift heavy ion irradiation and will be discussed from the point of view of extreme conditions created in the interaction with ions.

## Ceramic Spark Plug Electrodes for Large Gas Engine Applications

**Manuel Gruber<sup>1</sup>, Walter Harrer<sup>1</sup>, Raul Bermejo<sup>1</sup>, Anton Tiltz<sup>2</sup>,  
Wolfgang Fimml<sup>3</sup>, Andreas Wimmer<sup>4</sup>**

<sup>1</sup>*Department Materials Science, Chair of Structural and Functional Ceramics,  
Montanuniversität Leoben, Peter-Tunner-Strasse 5, 8700 Leoben, Austria*

<sup>2</sup>*LEC GmbH Graz, Inffeldgasse 19, 8010 Graz, Austria*

<sup>3</sup>*Innio Jenbacher GmbH & Co OG, Achenseestrasse 1-3, 6200 Jenbach, Austria*

<sup>4</sup>*Institute of Thermodynamics and Sustainable Propulsion Systems, Graz, University of Technology,  
Inffeldgasse 19, 8010 Graz*

The research on large gas engines is driven by ever higher requirements regarding efficiency and emissions. The extreme conditions in the combustion chamber towards higher pressures and temperatures significantly increase the wear of spark plug electrodes.

Currently used expensive rare-metals are reaching their limits in terms of resilience to wear, thus alternative materials are sought to increase maintenance intervals and engine reliability. In this context, advanced ceramics seem to be interesting candidate materials due to their often high thermal stability, excellent oxidation and corrosion resistance at high temperatures together with better availability of raw materials at lower cost than conventionally used rare-metals.

This publication provides insights into the material selection process together with promising preliminary results for several ceramic alternatives to existing spark plug electrode materials. Nevertheless, their inherent brittleness may compromise the applicability due to (thermo-) mechanical stresses, which may arise during the manufacturing process, handling or service. Therefore, mechanical characterization has been employed in order to estimate tolerable stress limits and to get an understanding of the dominating loading conditions that may lead to fracture of the investigated materials.

## **Ultra fast laser processing of materials for science and industry**

**Branislav Jelenković**

*Institute of Physics, University of Belgrade, Belgrade, Serbia*

Processing of materials with focused femtosecond (fs) laser pulses is advancing towards various applications due to unique characteristics of its 3D two-photon lithography and direct multi-photon material ablation. High peak power delivered during ultra short pulses, often of the order of several MW, allow fabrication of micron and submicron size structures because deposition of laser energy into electrons of the material is on a shorter time scale than the energy relaxation between electrons and lattice atoms – thus removing material before thermal diffusion in the bulk occurs. Two-photon interaction during a short laser pulse enables biological research and applications, development of optical memories with data density over  $10 \text{ Tbit cm}^{-3}$ , fabrication of 3D photonic crystals, spanning critical dimensions between 10 nm to 100  $\mu\text{m}$ . The latest achievements with fs lasers will be reviewed and some of emerging biomedical applications will be presented.

## **Thermal and chemical stability of boron nitride nanostructures**

**Claus Rebholz<sup>1</sup>, Nikolaos Kostoglou<sup>2</sup>, Branko Matovic<sup>3</sup>**

<sup>1</sup>*Department of Mechanical & Manufacturing Engineering, University of Cyprus, 1678 Nicosia, Cyprus*

<sup>2</sup>*Department of Materials Science, Montanuniversität Leoben, 8700 Leoben, Austria*

<sup>3</sup>*Vinča Institute of Nuclear Sciences, University of Belgrade, 11000 Belgrade, Serbia*

In recent years, there has been a great interest in the synthesis and application of boron nitride (BN) nanomaterials due to their unique physical, chemical and mechanical properties. Much attention has been drawn towards nanoscale h-BN, among the most promising inorganic nanomaterials. In this study, the texture/porosity, structure, surface chemistry, morphology and elemental composition of h-BN nanoplatelets and nanotubes were evaluated and compared to carbon-based materials with similar structures. The experimental results showed superior high temperature stability for the h-BN nanomaterials and revealed which of the evaluated materials demonstrated the best high-temperature performance/resistance, therefore allowing the correlation of oxidation behaviour with specific structural features (e.g. crystallinity, specific surface area, particle shape).



## Sintering properties of heavily Bi-doped CeO<sub>2</sub>

**Marija Prekajski Đorđević<sup>1</sup>, Branko Matović<sup>1</sup>, Jelena Maletaškić<sup>1</sup>, Jelena Erčić<sup>1</sup>, R. Subasri<sup>2</sup>**

<sup>1</sup>*Institute of Nuclear Sciences "Vinca", Belgrade University, Belgrade, Serbia*

<sup>2</sup>*Centre for Nanotechnology, Central University of Jharkhand, Brambe, Ranchi-835205, India*

Ceria-based materials have been extensively studied as one of the most promising electrolytes for reduced temperature solid oxide fuel cell (SOFC) system due to their high ionic conductivity at moderate temperature [1-3]. CeO<sub>2</sub> system doped with Bi<sup>3+</sup> can be very interesting for application in SOFC's due to the high ion conductivity of CeO<sub>2</sub> and Bi<sub>2</sub>O<sub>3</sub> phases. Cost and time effective Self Propagating Room Temperature procedure (SPRT) was used as synthesis method of heavily Bi doped CeO<sub>2</sub> nanopowders, with up to 50% of Bi<sup>3+</sup>. The results obtained by XRPD accompanied with Rietveld refinement analysis show that all samples were single-phase solid solution at room temperature with chemical formula Ce<sub>1-x</sub>Bi<sub>x</sub>O<sub>2-δ</sub> where x = 0.1 - 0.5. Transmission electron microscopy (TEM) showed that average crystallite size of synthesized powders was less than 5 nm. Synthesized samples were sintered with two different methods - Conventional (CS) and Microwave (MS). Powders were densified by sintering at different temperatures, in an air atmosphere for 1 h. It appears that conventional sintering requires much higher temperatures for densification. However, at high temperatures there is significant loss of Bi<sup>3+</sup> content due to process of evaporation. This problem can be overcome by applying the microwave sintering technique. In this way high densified samples can be obtained at much lower temperatures (1050 °C) without loss of Bi<sup>3+</sup> concentration.

# **POSTER PRESENTATIONS**

## ESR analysis of Mn<sup>2+</sup> cations at temperatures of 4.2-293 K in kerogen isolated from graptolitic black shale at Zvonačka Banja (Zvonce, Eastern Serbia)

Bratislav Todorović<sup>1</sup>, Pavle I. Premović<sup>2</sup>, Dragan T. Stojilković<sup>1</sup>, Sreten B. Stojanović<sup>1</sup>

<sup>1</sup>Faculty of Technology, University of Niš, Serbia

<sup>2</sup>Laboratory for Geochemistry, Cosmochemistry and Astrochemistry, University of Niš, Serbia

The Zvonce graptolitic shale is believed to have been deposited under stagnant anoxic conditions in a sheltered area of a shallow epicontinental sea (Silur). The kerogen isolation procedure from it is similar to that used by Premović et al.<sup>1</sup>. Spectra were recorded on a Bruker ER-200 series ESR spectrometer. The X-band/Q-band measurements were made at 9.4 GHz and 35 GHz. A measurements were carried out at different temperatures using a nitrogen-flow device for cooling. Spectra at liquid nitrogen temperature of 77 K were obtained using a Bruker dewar. Liquid helium measurements at temperature of approximately 4.2 K were made on a Bruker ESP-380E spectrometer equipped with an Oxford Instruments helium-flow cryostat. All ESR measurements are performed in the laboratories of Université Pierre & Marie Curie (UPMC) by Premović.

The spectra exhibit the six-line pattern with a high g factor of  $2.154 \pm 0.005$  and an isotropic hyperfine constant (A) of  $7.56 \pm 0.1$  mT. These six lines are identical but asymmetric at all temperatures and microwave bands (X and Q). For the sake of clarity, Figure 1 shows only the Q-band spectrum of the Mn<sup>2+</sup> resonance at 151 K. This cation was not detected in kerogen from room temperature down to about 250 K. A computer simulation revealed that the line asymmetry is probably due to the superposition of the two (or possibly more) very similar Lorentzians for different Mn<sup>2+</sup> sites. These sites are probably very similar but not identical. In general, the covalency (or ionicity) of the bond between Mn<sup>2+</sup> and ligands can be very roughly estimated using Matumura's plot.<sup>2</sup> Using value obtained from the ESR spectrum of the Mn<sup>2+</sup> studied  $A=7.56$  mT (or  $76 \times 10^{-4} \text{ cm}^{-1}$ ) we estimated a low covalency of about 15 %. Furthermore, this splitting would suggest that Mn<sup>2+</sup> is probably bonded to oxygen or sulfur atoms of the ligands in sixfold coordination.<sup>3</sup> Stepwise heating from about 4.2 K up to about 245 K led to an increase in the line width  $\Delta H_p-p(T)$ . Figure 3 shows the dependence of  $\Delta H(T)$  (i.e.,  $1/T_1$ ) on temperature in a log-log graph. This dependence indicates that the relaxation time is proportional to  $T^{-2}$  for temperatures above 77 K. Such behavior is characteristic of a Raman relaxation process.

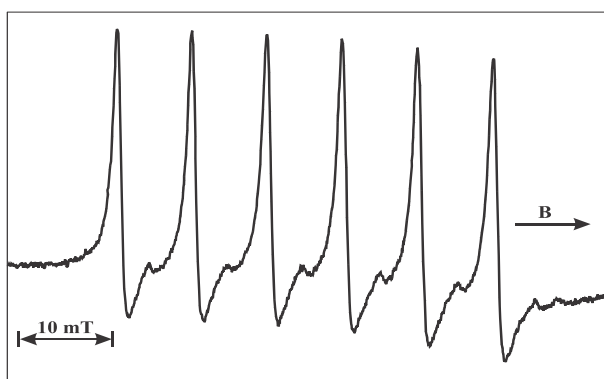


Figure 1. Narrow-range ESR spectrum of Mn<sup>2+</sup> in the Zvonce kerogen at 151 K.

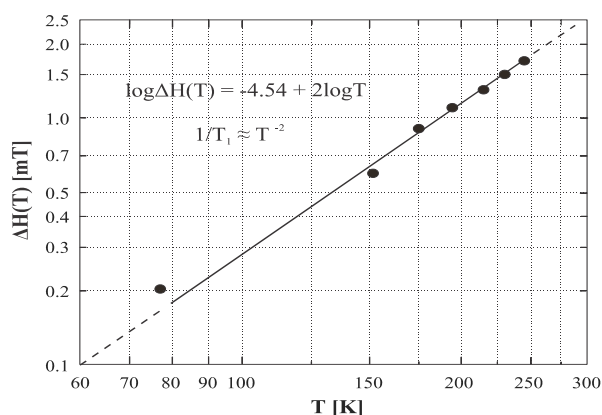


Figure 2. Plot of the spin-phonon part of the ESR line width  $\Delta H_p-p$  vs temperature T (log-log scale) for Mn<sup>2+</sup>.

### References

- [1] P. Premović, Lj. Jovanović, G. Popović, N. Pavlović, M. Pavlović, J Serb Chem Soc, 53 (1988) 427.
- [2] O. Matumura, Phys. Soc. Jpn, 14 (1959) 108.
- [3] J. Wertz, J. Bolton, McGraw-Hill, New York, 1972.

## DFT study of structural stability and mechanical properties: High-Entropy Alloys (HEAs) - Ultra-High Temperature Ceramics (UHTC)

**Dejan Zagorac<sup>1,2</sup>, Ivana Cvijović-Alagić<sup>1,2</sup>, Jelena Zagorac<sup>1,2</sup>, Svetlana Butulija<sup>1,2</sup>, Jelena Erčić<sup>1,2</sup>, Ondrej Hanzel,<sup>3</sup> Richard Sedlák,<sup>4</sup> Maksym Lisnichuk,<sup>5</sup> Tamara Škundrić<sup>1,2</sup>, Milan Pejić<sup>1,2</sup>, Dušica Jovanović<sup>1,2</sup>, Peter Tatarko,<sup>3</sup> Branko Matović<sup>1,2</sup>**

<sup>1</sup>*Materials Science Laboratory, Institute of Nuclear Sciences “Vinča”, University of Belgrade, Belgrade, Serbia*

<sup>2</sup>*Center for synthesis, processing, and characterization of materials for application in the extreme conditions “CextremeLab”, Belgrade, Serbia*

<sup>3</sup>*Institute of Inorganic Chemistry, Slovak Academy of Sciences, Dúbravská cesta 9, 84536 Bratislava, Slovak Republic*

<sup>4</sup>*Institute of Materials Research, Slovak Academy of Sciences, Watsonova 47, 04001 Košice, Slovak Republic*

<sup>5</sup>*Faculty of Science, Institute of Physics, Pavol Jozef Šafárik University in Košice, Park Angelinum 9, 04001 Košice, Slovak Republic*

High-Entropy Alloys (HEAs) have attracted considerable interest due to the combination of useful properties and enhanced applications, and a few HEAs have already been shown to possess exceptional properties under extreme conditions (e.g. Ultra-High Temperature Ceramic (UHTC)). However, predicting the formation, structures, and stability of HEAs is one of the major goals of recent studies, which is expected to bring discovery of new systems with enhanced properties of the material, with special attention on high temperature and mechanical load. Here, we show an example of high-entropy rare-earth (RE) zirconates with a pyrochlore structure that was examined theoretically and experimentally observed. Theoretical methods were applied to investigate the variable composition of the ordered and disordered pyrochlore structures using quantum mechanics, group action theory, PCAE, and supercell methods. The investigated RE<sub>2</sub>Zr<sub>2</sub>O<sub>7</sub> compound was successfully fabricated by pressureless and spark plasma sintering, with nominal composition (La<sub>0.2</sub>Y<sub>0.2</sub>Gd<sub>0.2</sub>Nd<sub>0.2</sub>Sm<sub>0.2</sub>)Zr<sub>2</sub>O<sub>7</sub>, prepared by simple glycine nitrate procedure (GNP) and characterized using various experimental methods (XRD, SEM, TEM, Raman, etc.). [1] Pyrochlore structures were generated using the Primitive Cell Approach for Atom Exchange (PCAE) method [2] or the supercell approach using the Crystal17 program package [3], and investigation of disordered systems and solid solutions was conducted using the group action theory [4]. Structural optimization on the *ab initio* level was performed using the Crystal17 code, based on a Linear Combination of Atomic Orbitals (LCAO). Density functional theory (DFT) calculations were utilized in the present study, using the local density approximation (LDA) with Perdew–Zunger (PZ) correlation functional.

### References

- [1] B. Matović, D. Zagorac, I. Cvijović-Alagić, J. Zagorac, S. Butulija, J. Erčić, O. Hanzel, R. Sedlák, M. Lisnichuk, P. Tatarko, Fabrication and characterization of high entropy pyrochlore ceramics, *Boletín de la Sociedad Española de Cerámica y Vidrio* (2021).
- [2] D. Zagorac, J. Zagorac, J.C. Schön, N. Stojanovic, B. Matovic, ZnO/ZnS (hetero) structures: ab initio investigations of polytypic behavior of mixed ZnO and ZnS compounds, *Acta Crystallogr. Sect. B: Struct. Sci. Cryst. Eng. Mater.* 74 (2018) 628–642.
- [3] R. Dovesi, F. Pascale, B. Civalleri, K. Doll, N.M. Harrison, I. Bush, P. D’arco, Y. Noël, M. Rérat, P. Carbonniere, The CRYSTAL code 1976-2020 and beyond, a long story, *J. Chem. Phys.* 152 (2020) 204111.
- [4] S. Mustapha, P. D’Arco, M. De La Pierre, Y. Noël, M. Ferrabone, R. Dovesi, On the use of symmetry in configuration analysis for the simulation of disordered solids, *J. Phys.:Condens. Matter* 25 (2013) 105401.

## Structural, electronic and mechanical properties of bulk B<sub>4</sub>C from first principles

**Dušica Jovanović<sup>1,2</sup>, Jelena Zagorac<sup>1,3</sup>, Dejan Zagorac<sup>1,3</sup>, Branko Matović<sup>1,3</sup>**

<sup>1</sup>*Institute of Nuclear Sciences Vinča, Materials Science Laboratory, University of Belgrade, 11000 Belgrade, Serbia*

<sup>2</sup>*Department of Chemistry, Faculty of science and mathematics, University of Nis, 18000 Nis, Serbia*

<sup>3</sup>*Center for Synthesis, Processing and Characterization of Materials for Application in the Extreme Conditions-CextremeLab, 11000 Belgrade, Serbia*

Boron carbide (B<sub>4</sub>C, space group no. 166) has attracted great attention as a semiconducting material with excellent properties and have found various technological applications. The high hardness value makes it a potentially superhard material as well as a low density, high degree of chemical inertness, high melting temperature, thermal stability, abrasion resistance, and excellent neutron absorption, contributed to the use of boron carbide as an abrasive material for extreme conditions, wear resistance components, body armors and as a nuclear absorber or solid state neutron detector. However, B<sub>4</sub>C is known for its unusual structure, bonding, and substitutial disordering whose nature is not yet fully understood, and exhibits brittle impact behavior. The most theoretically obtained structures of the 15-atom periodic unit cell are the chain-, polar-, and equatorial-model of solid boron carbide. In this study we investigated the chain-model structure with an arrangement of 12-boron atom icosahedra and linear 3-carbon atom chains (Figure 1), using available experimental data from the ICSD database. We employed the DFT method with LDA and GGA-PBE functional, as implemented in the CRYSTAL17 software package.

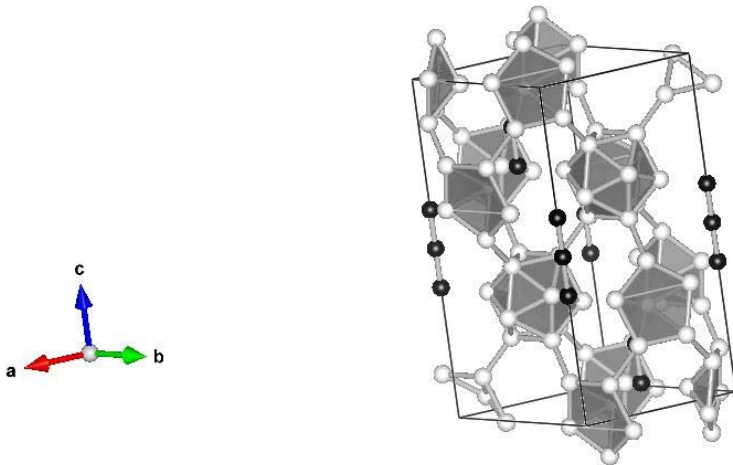


Figure 1. Unit cell of chain-model rhombohedral B<sub>4</sub>C visualized by the VESTA program.

Calculated equilibrium energies obtained by both functionals had similar values, and optimized unit cell parameters and interatomic distances are in a good agreement with initial experimental data. Electronic properties of boron carbide have been investigated by calculating density of states (DOS) and band structure. Calculated mechanical properties: bulk modulus, shear modulus, Young modulus, Poisson's ratio, hardness and elastic tensor constants showed mechanical stability of B<sub>4</sub>C, while the hardness value of 36.54 GPa calculated by LDA functional showed an excellent agreement with available experimental data, while GGA-PBE calculations of bulk modulus and Poisson's ratio showed values closest to the experimentally measured.

## Anion substitution and the structure-property influence of sulfur on mixed TiO<sub>2</sub>/TiS<sub>2</sub> compounds

**Dušica Jovanović<sup>1,2</sup>, Dejan Zagorac<sup>1,3</sup>, Branko Matović<sup>1,3</sup>, Milan Pejić<sup>1,3</sup>, Tamara Škundrić<sup>1,3</sup>, Jelena Zagorac<sup>1,3</sup>**

<sup>1</sup>*Institute of Nuclear Sciences Vinča, Materials Science Laboratory, University of Belgrade, 11000 Belgrade, Serbia*

<sup>2</sup>*Department of Chemistry, Faculty of science and mathematics, University of Nis, 18000 Nis, Serbia*

<sup>3</sup>*Center for Synthesis, Processing and Characterization of Materials for Application in the Extreme Conditions-CextremeLab, 11000 Belgrade, Serbia*

Recent studies of TiO<sub>2</sub>/TiS<sub>2</sub> nanostructures with various morphologies have been reported, usually showing improved properties with applications from electronics and catalysis to solar cells and medicine. However, there is a limited number of studies on the crystal structures of TiO<sub>2</sub>/TiS<sub>2</sub> compounds with corresponding properties. In order to investigate TiO<sub>2</sub>/TiS<sub>2</sub> mixed compounds as a function of sulfur doping, *ab initio* modelling using DFT method has been performed. In particular, solid solutions of TiO<sub>1-x</sub>S<sub>x</sub> ( $x = 0, 0.25, 0.5, 0.75$  and  $1$ ) with anatase, rutile, and CdI<sub>2</sub> crystal structures were investigated using LDA-PZ and GGA-PBE functionals. Novel phase transitions and predicted structures are presented, and apart from several interesting metastable structures, a very interesting pressure-induced phase transition is found in the TiOS compound (Figure 1). Furthermore, electronic properties were studied through the dependence of semiconducting properties on dopant concentration. The first description of the electronic properties of the mixed TiO<sub>1-x</sub>S<sub>x</sub> compounds in crystal form has been presented, followed by a detailed study of the structure-property relationship, which will possibly have numerous industrial and technological applications.

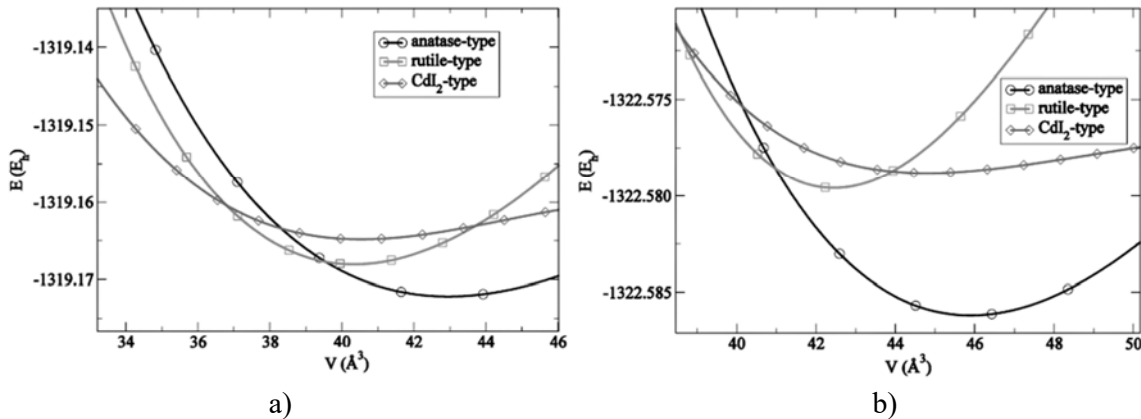


Figure 1. Energy-volume curves for TiOS composition with anatase, rutile, and CdI<sub>2</sub> structure type calculated using a) LDA-PZ and b) GGA-PBE functional, respectively.

## Laser desorption/ionization mass spectrometry of $\text{Li}_{1.999}\text{Ta}_{0.005}\text{SiO}_3$

**Filip Veljkovic<sup>1</sup>, Branko Matovic<sup>1</sup>, Svetlana Butulija<sup>1</sup>, Milovan Stoilkovic<sup>1</sup>, Ivana Stajcic<sup>1</sup>,  
Bojan Jankovic<sup>1</sup>, Suzana Velickovic<sup>1</sup>**

<sup>1</sup>*University of Belgrade, "Vinča" Institute of Nuclear Sciences - National Institute of the Republic of Serbia, Mike Petrovića Alasa 12-14, P.O. Box 522, 11001 Belgrade, Republic of Serbia*

In the last couple of decades the scientific is making great efforts to investigate the phenomenon of laser-matter interaction, because these knowledge can directly positively influence on technological innovations in the field of materials. This phenomenon are still not fully invetigate since involves a number physical and chemical processes, which take place simultaneously or separated in time and space [1]. The laser desorption/ionization (LDI) implies the following processes: the laser provide a pulse of energy to sample (for a few ns), the sample increases in temperature quickly ( to several thousand degrees), so lead to the production ions, neutrals and electrons in the gass phase [2].

The aim of this paper is to examine the products of the gas phase formed during the interaction of laser-  $\text{Li}_{1.999}\text{Ta}_{0.005}\text{SiO}_3$ . The  $\text{Li}_{1.999}\text{Ta}_{0.005}\text{SiO}_3$  ceramics has a wide application because the melting of lithium metasilicate is used for the calibration of thermocouples, as a flux in glazes and ceramic enamels, dental glass, nuclear waste immobilization as well as ceramic materials for fusion reactors. The knowledge gained should contribute to a better understanding behavior of  $\text{Li}_{1.999}\text{Ta}_{0.005}\text{SiO}_3$  in extreme conditions.

The experiments were performed on a commercial matrix-assisted laser desorption/ionization mass spectrometer (MALDI MS) with time of flight mass analyzer (Voyager-DE PRO, Sciex, USA), equipped with a nitrogen pulse laser (pulse duration of 3 ns, 20 Hz, and wavelength of 337 nm). The mass spectra were obtained using the LDI (without matrices) positive and negative reflector modes.

It is known that the LDI MS is an efficient method for the production and detection of homogeneous and heterogeneous clusters [3]. Preliminary results shows that the ion signals in the negative ion LDI mass spectrum of  $\text{Li}_{1.999}\text{Ta}_{0.005}\text{SiO}_3$  correspond to the following species:  $m/z$  59.89  $\text{SiO}_2^-$  (calcd 59.97),  $m/z$  71.90  $\text{Si}_2\text{O}^-$  (calcd 71.95),  $m/z$  83.90  $\text{Si}_3^-$  (calcd 83.93),  $m/z$  95.91  $\text{Si}(\text{OH})_4^-$  (calcd 95.99),  $m/z$  107.91  $\text{Si}_2(\text{OH})_2(\text{H}_2\text{O})^-$  (calcd 107.97),  $m/z$  119.92  $\text{Si}_2\text{O}_4^-$  (calcd 119.93),  $m/z$  120.95  $\text{Si}_2\text{O}_3(\text{OH})^-$  (calcd 120.94),  $m/z$  131.93  $\text{Si}_3\text{O}_3^-$  (calcd 131.92),  $m/z$  143.92  $\text{Si}_2(\text{OH})_2(\text{H}_2\text{O})_3^-$  (calcd 143.99). The ion signals in the positive mode were attributed to the following cations:  $\text{LiSi}(\text{OH})^+$  ( $m/z$  52.02, calcd 51.99),  $\text{Li}_3(\text{OH})(\text{H}_2\text{O})^+$  ( $m/z$  56.04, calcd 56.06),  $\text{Li}_2\text{SiO}^+$  ( $m/z$  58.05 calcd 58.00),  $\text{Li}_3\text{Si}_2\text{H}_2(\text{H}_2\text{O})^+$  ( $m/z$  97.15 calcd 97.03),  $\text{Li}_5\text{Si}_2\text{H}_2\text{O}^+$  ( $m/z$  109.10, calcd 109.04).

The results show that silicon-oxygen cluster ions were formed in the negative mode, while lithium-silicon clusters were detected in the positive mode.

### Acknowledgements

Authors would like to acknowledge financial support of Ministry of Education, Science and Technological Development of the Republic of Serbia, under Contract numbers 451-03-068/2022-14/200017.

### References

- [1] N. Bulgakova, A. Panchenko, V. Zhukov, S. Kudryashov, A. Pereira, W. Marine, T. Mocek, and A. Bulgakov, *Micromachines* 2014, 5, 1344-1372; doi:10.3390/mi5041344.
- [2] D. Lubman, *Lasers and Mass Spectrometry*, Oxford University Press, New York (1990)
- [3] J. McIndoe, *Transition Metal Chemistry*, 28, 122-131 (2003)

## Hydrogen peroxide-assisted route for nanocrystalline WO<sub>3</sub> synthesis with excellent sensing response

**Jelena Erčić**, Dejan Zagorac<sup>1</sup>, Olga Ivanova<sup>2</sup>, Alexander Baranchikov<sup>2,3</sup>, Taisiya Shekunova<sup>2,3</sup>, Khursand Yorov<sup>2,3</sup>, Olga Gajtko<sup>2</sup>, Lili Yang<sup>3</sup>, Marina Rumyantseva<sup>3</sup>, Vladimir Ivanov<sup>2</sup>, Branko Matović<sup>1</sup>

<sup>1</sup> Vinča Institute of Nuclear Sciences, National Institute of the Republic of Serbia, University of Belgrade, Belgrade, Serbia

<sup>2</sup> Kurnakov Institute of General and Inorganic Chemistry of the Russian Academy of Sciences, Moscow, Russia

<sup>3</sup> Lomonosov Moscow State University, Moscow, Russia

<sup>4</sup> National Research Tomsk State University, Tomsk, Russia

This research indicates great NO<sub>2</sub>-sensing properties of tungsten oxide nanoparticles, prepared through a simple method consisting of dissolution of elementary tungsten in a mixture of hydrogen peroxide, 2-propanol, and water, followed by low-temperature (400°C) heating. Through a comprehensive literature study on sensor properties of tungsten oxide prepared in different ways, it was found that the sensor response towards NO<sub>2</sub> obtained in this work achieved the highest level. A remarkable characteristic of the obtained powder was a highly reproducible sensor signal at room temperature, more than 100 times higher than any previously described for WO<sub>3</sub>. The probable reason for this high sensor response was the presence of two WO<sub>3</sub> polymorphs ( $\gamma$ -WO<sub>3</sub> and  $h$ -WO<sub>3</sub>) in the obtained material. In further investigation of synthesized WO<sub>3</sub> materials, experimental (XRD, SEM, TEM, BET) and theoretical (B3LYP, HSE) methods have been used, along with the resistance and sensor response measurements at various temperatures.

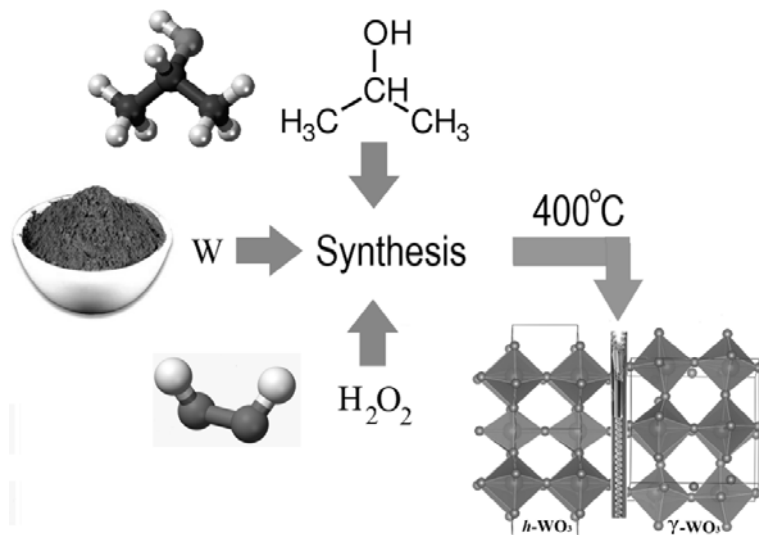


Figure 1. Schematic representation of experimental synthesis of crystalline WO<sub>3</sub> nanoparticles



## Crystal structure and properties of theoretically predicted *c*-AlB<sub>12</sub>

**Jelena Zagorac<sup>1,2</sup>, Dušica Jovanović<sup>1,3</sup>, Dejan Zagorac<sup>1,2</sup>, Tamara Škundrić<sup>1,3</sup>, Milan Pejić<sup>1,4</sup>,  
Branko Matović<sup>1,2</sup>**

<sup>1</sup>*Materials Science Laboratory, Institute of Nuclear Sciences “Vinča”, University of Belgrade, Belgrade, Serbia*

<sup>2</sup>*Center for synthesis, processing, and characterization of materials for application in the extreme conditions “CextremeLab”, Belgrade, Serbia*

<sup>3</sup>*Department of chemistry, Faculty of science and mathematics, University of Nis, Nis, Serbia*

<sup>4</sup>*Faculty of Physics, University of Belgrade, Belgrade, Serbia*

Aluminum borides have various industrial applications, used in fuels, explosives, abrasives, and as additives to consolidated materials based on boron carbide. The structure of AlB<sub>12</sub> is similar to that of boron carbide, including almost regular icosahedrons of boron atoms. The absence of the structure data of some higher aluminum borides and the presence of a large number of reflexes in their diffraction patterns makes the identification of phase compositions very difficult and limits the possibilities of the computer modeling of the AlB<sub>12</sub>. The crystal structure of AlB<sub>12</sub> is usually considered as tetragonal  $\alpha$ -AlB<sub>12</sub> (space group  $P4_32_12$ ) and orthorhombic  $\gamma$ -AlB<sub>12</sub> (space group  $P2_12_12_1$ ) which can be synthesized from high-temperature Al-B melts.

In our work, we have performed *ab initio* optimization of the  $\alpha$ -AlB<sub>12</sub> using GGA-PBE functional and obtained relaxed unit cell parameters and atomic positions. Furthermore, we have relaxed AlB<sub>12</sub> composition starting from the UB<sub>12</sub> structure type. The new cubic phase *c*-AlB<sub>12</sub> crystallizes in the space group  $Fm-3m$  and has a better total energy ranking than  $\alpha$ -AlB<sub>12</sub> on the GGA-PBE level of theory. Also, for the new *c*-AlB<sub>12</sub>, we have calculated electronic and mechanical properties on different pressures and made the comparison with available experimental data in the AlB<sub>12</sub> system.

## Influence of temperature on corrosion of high purity alumina ceramics in acidic aqueous solution

Ivana Ropuš<sup>1</sup>, Lidija Ćurković<sup>1</sup>, Sanda Rončević<sup>2</sup>, Ivana Gabelica<sup>1</sup>

<sup>1</sup>*Energoatest zaštita d.o.o., Potočnjakova 4, 10000 Zagreb*

<sup>2</sup>*Faculty of Mechanical Engineering and Naval Architecture, University of Zagreb, Ivana Lučića 5, 10000, Zagreb*

<sup>3</sup>*Faculty of Science, University of Zagreb, Horvatovac 102a, 10000 Zagreb, Croatia*

Developing ceramic materials with resistance to various chemicals as well as certain mechanical characteristics is of considerable importance for enabling a wider application of these ceramics [1]. Chemical resistance depends on the purity and microstructure of the material along with the kind of the aggressive medium and temperature [2,3]. For this reason, alumina ceramics of 99,8 % purity has been prepared. The rest are impurities (CaO, Na<sub>2</sub>O, SiO<sub>2</sub> and Fe<sub>2</sub>O) and MgO as sintering aid. The two main types of chemical resistance of ceramics are: acid and alkali resistance. Despite the fact that ceramics are generally more stable in corrosive environments than common metallic materials are, it is important to investigate the chemical resistance under a range of conditions – from highly corrosive conditions, for example in strong acid and a long period of exposure to mildly corrosive conditions. Consequentially, the corrosion behavior of cold isostatically pressed (CIP) high purity alumina ceramics in aqueous HNO<sub>3</sub> solutions in a concentration range of 0.50 mol dm<sup>-3</sup>, 1.25 mol dm<sup>-3</sup> and 2.00 mol dm<sup>-3</sup> with different exposure times – up to 10 days – has been studied. The influence of temperature (25, 40 and 55 °C) on corrosion was also monitored in the solutions of the lowest concentration of HNO<sub>3</sub> (0.5 mol/L) with an exposure time of 48 hours. The results were obtained by determining the mass concentration of Al<sup>3+</sup>, Mg<sup>2+</sup>, Ca<sup>2+</sup>, Na<sup>+</sup> Si<sup>4+</sup> and Fe<sup>3+</sup> ions eluted in the HNO<sub>3</sub> aqueous solution by means of inductively coupled plasma optical emission spectrometry (ICP-OES) as well as comparing weight changes in every sample before and after exposure to the corrosive mediums, measured by an analytical balance with the degree of precision of 10<sup>-5</sup> g.

### Acknowledgments:

This research was funded by the Croatian Science Foundation under the project Monolithic and composite advanced ceramics for wear and corrosion protection (WECOR) (IP-2016-06-6000).

### References

- [1] I. Žmak, D. Ćorić, V. Mandić, L. Ćurković, Hardness and Indentation Fracture Toughness of Slip Cast Alumina and Alumina-Zirconia Ceramics, *Materials*, 13 (2020) 1- 17.
- [2] S. Kurajica, V. Mandić, L. Ćurković, Mullite ceramics acid corrosion kinetics as a function of gel homogeneity, *Biointerface Research in Applied Chemistry*, 7 (2017) 2295-2299.
- [3] Ronald A. McCauley, *Corrosion of Ceramic Materials*, Taylor & Francis, 2017

## **Investigation of Yb<sup>3+</sup>/Er<sup>3+</sup> doped SrGd<sub>2</sub>O<sub>4</sub> up-conversion nanomaterial obtained via combustion synthesis**

**Tijana Stamenković, Nadežda Radmilović, Maria Čebela, Marija Prekajski Đorđević, Vesna Lojpur**

*Vinča Institute of Nuclear Sciences, National Institute of the Republic of Serbia, P.O. Box 522,  
11001 Belgrade, University of Belgrade, Serbia*

Nanopowders of a new up-conversion materials, SrGd<sub>2</sub>O<sub>4</sub> co-doped with different Yb<sup>3+</sup> (1, 2.5 and 5 at%) and constant Er<sup>3+</sup> (0.5 at%) concentrations were prepared by combustion method. X-ray powder diffraction (XRPD) showed that nanoparticles have orthorhombic structure (Pnma), assigned to the JCPDS Card No:01-072-6387. Rietveld refinement indicated a decrease in the size of the unit cell, lattice parameters, and cell volume, due to successful doping of Yb<sup>3+</sup> and Er<sup>3+</sup> ions into the host structure. Transmission electron microscopy (TEM) revealed that obtained nanostructure is composed of agglomerated nanoparticles, while energy dispersive spectroscopy (EDS) confirmed uniform distribution of all constituting elements in them. Up-conversion (UC) luminescence spectra measured in function of laser pumping power indicated that two-photon UC process is established in nanoparticles as a result of the trivalent erbium f-f electronic transitions: two green emission bands at 523 and 551 nm (<sup>2</sup>H<sub>11/2</sub>, <sup>4</sup>S<sub>3/2</sub> → <sup>4</sup>I<sub>15/2</sub>) as well as a red emission band at 661 nm (<sup>4</sup>F<sub>9/2</sub> → <sup>4</sup>I<sub>15/2</sub>). The rise of Yb<sup>3+</sup> concentration from 1 to 5 at% provokes a significant change of the green to red ratio showing the ability to fine-tuning the color output.

## **Synthesis and characterization of a new Dy<sup>3+</sup> and Sm<sup>3+</sup> doped SrGd<sub>2</sub>O<sub>4</sub> down-conversion nanomaterial obtained via glycine-assisted combustion synthesis**

**Tijana Stamenković, Nadežda Radmilović, Jelena Erčić, Maria Čebela, Vesna Lojpur**

*Vinča Institute of Nuclear Sciences, National Institute of the Republic of Serbia, P.O. Box 522,  
11001 Belgrade, University of Belgrade, Serbia*

In this investigation, down-conversion nanopowders of SrGd<sub>2</sub>O<sub>4</sub> doped with different concentrations of either Dy<sup>3+</sup> or Sm<sup>3+</sup> ions were examined. All samples were prepared via glycine-assisted combustion method, first burned at 500 °C for 1.5h and additionally calcined at 1000 °C for 2.5h, at ambient room temperature. The XRD analysis confirmed that all samples crystallize as single phase and the orthorhombic lattice SrGd<sub>2</sub>O<sub>4</sub>. TEM analysis determined high degree of crystallinity of samples with grain size of approximately 200 nm for Dy<sup>3+</sup> doped and 150 nm for Sm<sup>3+</sup> doped SrGd<sub>2</sub>O<sub>4</sub>. For both samples SAED showed that diffraction rings correspond to the *hkl* plane indices of SrGd<sub>2</sub>O<sub>4</sub>, while EDS indicated presence of Dy in crystal structure. Results of luminescent characterization demonstrated all appropriate emission peaks related to either Dy<sup>3+</sup> or Sm<sup>3+</sup> dopant ions. Investigation of dopant concentration revealed that the lowest values of both dopants have the most prominent emission peaks, while coordinates obtained from the CIE diagram showed emission shifting with the change of concentration.

## Mechanochemical activation of starting oxide mixtures for solid-state synthesis of BiFeO<sub>3</sub>

Maria Čebela<sup>1</sup>, Milena Rosić<sup>1</sup>, Vesna Lojpur<sup>2</sup>

<sup>1</sup>Center of Excellence “CEXTREME LAB”, Institute of Nuclear Sciences “Vinča”, University of Belgrade, Serbia

<sup>2</sup>Department of Atomic Physics, Institute of Nuclear Sciences “Vinča”, University of Belgrade, Serbia

Bismuth ferrite (BiFeO<sub>3</sub>) is one of the most researched single-phase multiferroic materials. The Fe<sub>2</sub>O<sub>3</sub> and Bi<sub>2</sub>O<sub>3</sub> oxides were the starting materials for the synthesis of the single phase BiFeO<sub>3</sub>. The preparation of BiFeO<sub>3</sub> was done by solid-state method with slight innovation: first, the oxides were activated separately, not together as usual, by milling in the ball mill and second, the 1% oleic acid was added to Bi<sub>2</sub>O<sub>3</sub> as a surfactant before milling, to prevent its granulation. The adding of the oleic acid to Fe<sub>2</sub>O<sub>3</sub> was not necessary, because it did not show granulation during milling. The activated Fe<sub>2</sub>O<sub>3</sub> and Bi<sub>2</sub>O<sub>3</sub> powders were characterized by granulometric analysis after milling in two steps for 4.5 h. The obtained particle sizes were confirmed by SEM micrographs. Finally, prepared oxide powders were mixed, homogenized and sintered. According to XRD pattern the final phase of Fe<sub>2</sub>O<sub>3</sub>-Bi<sub>2</sub>O<sub>3</sub> mixture sintered at 790°C for 4 hours was rhombohedral phase of the R3c space group (JCPDS No. 86-1518) BiFeO<sub>3</sub> with less than 4% of Bi-rich secondary phase of Bi<sub>25</sub>FeO<sub>40</sub>.

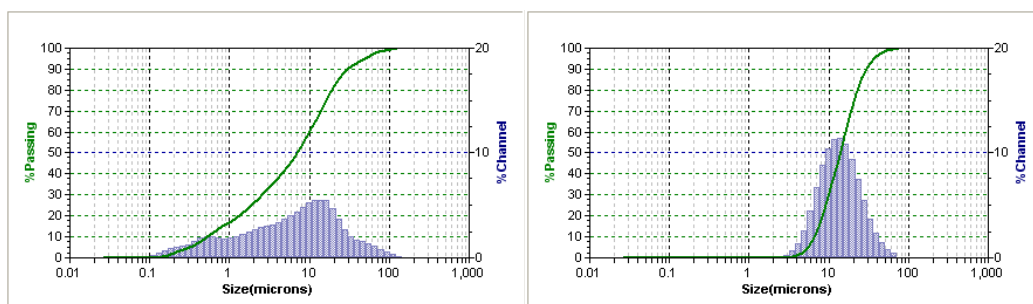


Figure 1. Particle size distributions of initial powders of a) Bi<sub>2</sub>O<sub>3</sub> and b) Fe<sub>2</sub>O<sub>3</sub>

## Energy landscape and crystal structure investigations of holmium(III) fluoro-selenide HoFSe

**Milan Pejić<sup>1,2</sup>, Dejan Zagorac<sup>1,2</sup>, Jelena Zagorac<sup>1,2</sup>, Tamara Škundrić<sup>1,2</sup>, Dušica Jovanović<sup>2</sup>,  
Branko Matović<sup>1,2</sup>**

<sup>1</sup>Materials Science Laboratory, Institute of Nuclear Sciences “Vinča”, University of Belgrade, Belgrade, Serbia

<sup>2</sup>Center for synthesis, processing and characterization of materials for application in the extreme conditions “CextremeLab”, Belgrade, Serbia

Ternary rare-earth metal compounds that contain fluorine and selenium (MFSe) crystallize into tetragonal PbFCl-type structures, with some trigonal and hexagonal exceptions. Also, new modifications with different properties may be found under different pressure and temperature conditions.

In order to theoretically predict new stable and/or metastable modifications of HoFSe, the following methods were used. First, global exploration was performed on energy landscape using simulated annealing with empirical potentials in software package G42+. Global optimization (GO) algorithm was applied to 4 fold (4Ho + 4F + 4Se; 12 atoms total) and 6 fold (6Ho + 6F + 6Se; 18 atoms total) formula units of HoFSe, and more than a million structure candidates were obtained this way. Structures were then symmetrized, grouped according to which space group they belong, and then compared with each other using an algorithm which we developed for this purpose (software package KPLOT is used as a module for the required operations). Structure types were then sorted by relevance criteria, such as ground state energy, number of found structures and symmetry. Afterwards, only a couple of hundred of relevant structure candidates remained. For them, local structural optimization was done on ab-initio level with different functionals (e.g. LDA, GGA-PBE and B3LYP) using CRYSTAL software package. Some of the found structure candidates with lowest ground state energy are shown in Figure 1.

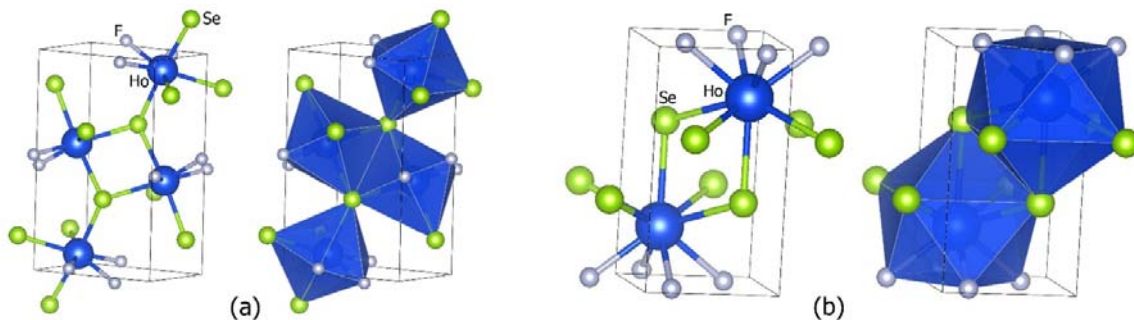


Figure 1. HoFSe structure types: (a) orthorhombic Pnma (space group 62), (b) tetragonal P4/nmm (space group 129).

Finally, E(V) (energy vs. volume) and H(p) (enthalpy vs. pressure) curves were calculated for several possible structure candidates in order to determine the stable phase at a given pressure and the transition pressures among the phases.

To better explore this class of ternary rare-earth compounds, further research on theoretical and experimental level is needed – e.g. measuring and calculating electronic, mechanical, optical, magnetic and other properties of compounds such as HoFSe. Also, performing global and local optimization with larger number of atoms is needed to find even more relevant structure candidates (such as polytypes).

## Theoretical study of ground state properties of Na<sup>+</sup>, Cs<sup>+</sup>, Mg<sup>2+</sup> and Ba<sup>2+</sup> doped mayenite and its electrider forms under extreme conditions

**Milan Pejić<sup>1,2</sup>, Dejan Zagorac<sup>1,2</sup>, Jelena Zagorac<sup>1,2</sup>, Tamara Škundrić<sup>1,2</sup>, Dušica Jovanović<sup>2</sup>, Branko Matović<sup>1,2</sup>**

<sup>1</sup>Materials Science Laboratory, Institute of Nuclear Sciences “Vinča”, University of Belgrade, Belgrade, Serbia

<sup>2</sup>Center for synthesis, processing and characterization of materials for application in the extreme conditions “CextremeLab”, Belgrade, Serbia

Mayenite (12CaO·7Al<sub>2</sub>O<sub>3</sub> or C12A7) is a complex nanoporous calcium-aluminum oxide that can capture large concentrations of extra-framework species inside its cages (Figure 1.) It crystallizes in the cubic crystal system belonging to the space group I-43d with lattice constant of about 12Å. Within its crystal lattice there are six interstitial sites that can accommodate the following ions: one oxide (O<sup>2-</sup>), two chloride (Cl<sup>-</sup>), two hydroxide (OH<sup>-</sup>), two hydride (H<sup>-</sup>), two fluoride (F<sup>-</sup>), one sulfide (S<sup>2-</sup>) or many other ones; some configurations give favorable encapsulation energy even for extra-framework cations of the first periodic table group. In case the all interstitial sites are empty, electrider (C12A7:2e<sup>-</sup>) is formed, with electron charge of 1/3e<sup>-</sup> per cage (2e<sup>-</sup> evenly distributed among six cages).

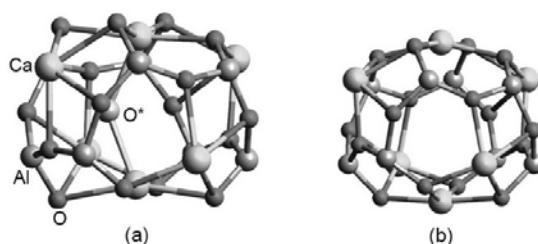


Figure 1. Mayenite cage with Ca-Al-O framework: (a) with inter-framework oxygen atom O\*, (b) without inter-framework species.

In this study we use ab-initio atomistic simulations to predict ground state properties – ground state energy, encapsulation energies of extra-framework species, electronic density of states and electronic band structure of C12A7 doped with selected cations from 1-st and 2-nd group of periodic table of elements. Calculations are performed at the density functional theory (DFT) level using Vienna Ab initio Simulation Package (VASP), Quantum Espresso (QE) and CRYSTAL packages.

Influence of interstitial doping and cationic substitution by the selected elements on structural and electronic features of C12A7, its electrider and partial electrider variants is studied under normal and extreme pressure conditions. Energy vs. volume, and enthalpy vs. pressure curves of these complex crystalline structures are determined in order to indicate stability and critical pressure of transformation between the configurations (e.g. transition from intra-framework Ca<sup>2+</sup>/extra-framework dopant to intra-framework dopant/extra-framework Ca<sup>2+</sup> configuration).

## Conventional and Unconventional Sintering of Alumina Ceramics

**Milan Vukšić<sup>1</sup>, Irena Žmak<sup>1</sup>, Lidija Ćurković<sup>1</sup>**

<sup>1</sup>*University of Zagreb, Faculty of Mechanical Engineering and Naval Architecture, Ivana Lučića 5,  
10000, Zagreb*

Corundum ( $\alpha$ -alumina) is one of the most exploited materials in the ceramic industry due to its low cost, and, importantly, due to excellent properties such as high strength and hardness, thermal stability, high wear resistance, and high chemical stability at elevated temperatures [1]. The goal of this paper is to explain the influence of the different sintering techniques on the properties of alumina ceramics, which contain a considerable amount of waste alumina powder. The study focused on the investigation of the conventional sintering and hybrid microwave sintering of alumina green bodies in which the grain growth and densification were characterized after sintering. The waste alumina powder, which is generated during machining of alumina green compacts and high-purity 99.99 % alumina powder ( $\alpha$ -Al<sub>2</sub>O<sub>3</sub>, Alcan Chemicals, USA), were used as starting materials. The stable concentrated aqueous alumina suspensions were prepared, and alumina green bodies were obtained by the slip casting method. The dried green samples were then conventionally sintered by using an electric furnace and by using a hybrid microwave sintering furnace. The used hybrid microwave sintering atmospheric furnace consists of a 2.45 GHz microwave generator with a continuously adjustable power output from 0 to 3 kW and external heating elements. The sintered samples exhibited higher density values and larger grain size for the conventional, one-step sintering, while for the hybrid microwave sintering lower density values and smaller grain size were observed. The slightly lower density values can be explained by the fact that alumina is a very poor microwave absorber [2], while smaller grain size can be explained by the fact that the rapid heating of microwave prevented grain size growth.

### **Acknowledgments:**

This research was funded by the Croatian Science Foundation under the project Monolithic and composite advanced ceramics for wear and corrosion protection (WECOR) (IP-2016-06-6000).

### **References**

- [1] Y. Pristinskiy, N. Washington Solis Pinargote, A. Smirnov, The effect of MgO addition on the microstructure and mechanical properties of alumina ceramic obtained by spark plasma sintering, *Materials Today: Proceedings*, 19 (2019) 1990-1993.
- [2] J. Wang, J. Binner, B. Vaidhyanathan, N. Joomun, J. Kilner, G. Dimitrakakis, T.E. Cross, Evidence for the Microwave Effect During Hybrid Sintering, *Journal of the American Ceramic Society*, 89 (2006) 1977-1984.



## **Water under extreme conditions: simultaneous gamma irradiation/carbon char adsorption resulted in improved methylene blue degradation**

**Radojka Vujašin, Ksenija Kumrić, Aleksandar Devečerski, Mia Omerašević, Marija Egerić, Đorđe Petrović, Ljiljana Matović**

*Vinča Institute of Nuclear Sciences, University of Belgrade, P. O. Box 522, 11001 Belgrade, Serbia*

Dyes and pigments are used by many industries to color their products. In this study, we applied two different kinds of waste materials: used radioactive sources and carbon waste tire char (WTC) to study their simultaneous effect of irradiation/adsorption on dye degradation. Irradiation of methylene blue (MB) by high energy  $\gamma$  radiation derived from used radioactive sources in the presence of carbon based material made of waste tire granules caused enhanced decoloration of the MB. Delivered dose of  $\gamma$  radiations differ depending on the type of isotope. The best decoloration was achieved using  $^{60}\text{Co}$  isotope. Complete decoloration of 20 ml of MB solution having concentration of  $100 \text{ mg dm}^{-3}$  of WTC was achieved with delivered dose of only 60 Gy. Decoloration of 90% was achieved after only 20 min while complete decoloration of MB solution (100%) was obtained in the irradiated samples after only 100 min.

Processes that use ionizing radiation ( $\alpha$ ,  $\beta$  and  $\gamma$ ) for decoloration of dyes are characterized as advanced oxidation processes which normally utilize a strong oxidizing species to break down the macromolecules. High energy radiation in water medium can produce radiolysis of water i.e. formation of several active species such as  $\text{H}_2$ ,  $\text{H}_2\text{O}_2$ ,  $\text{H}^+$ ,  $\text{OH}^-$ ,  $e_{\text{aq}}^-$ ,  $\bullet\text{OH}$  and  $\bullet\text{H}$  which are responsible for chemical reactions in water solutions. The significance of this approach is, except using waste materials for achieving enhanced degradation of organic pollutants in the solution, avoiding the need for safe disposal and storage of waste radioactive sources. Also, less waste material is generated at the end of the simultaneous irradiation/sorption process compared to the pure sorption process.

Surface composition of WTC, needed to elucidate the key mechanism of synergism of MB degradation, during the simultaneous adsorption/irradiation was obtained using FTIR and XPS technique.  $\text{OH}^-$  ions, that originate from radiolysis of water induced by gamma irradiation and from the surface of WTC, play the crucial role in degradation of MB. MB molecule adsorbed at the surface of WTC is electronically reorganized and as a consequence degraded via the opening of the central aromatic ring containing both heteroatoms, S and N.  $\text{OH}^-$  ions produced by water radiolysis also cause degradation of MB molecules in the solution. The synergetic effect is a result of the attack of  $\bullet\text{OH}$  radicals on electrostatic reorganized MB molecule adsorbed on surface of carbon material. Opening of central aromatic ring of MB firstly appeared in cleavage of the double  $\text{C-S}^+=\text{C}$  bond and then cleavage of double  $\text{N}=\text{C}$  bond.

## Solvothermal synthesis of zinc- and gallium-substituted cobalt ferrite nanoparticles

**Sonja Jovanović<sup>1</sup>, Marija Grujić<sup>1</sup>, Marko Jelić<sup>1</sup>, Marija Vukomanović<sup>2</sup>, Matjaž Spreitzer<sup>2</sup>,  
Marjeta Maček-Kržmanc<sup>2</sup>, Davide Peddis<sup>3,4</sup>**

<sup>1</sup>*Laboratory of Physics, Vinča Institute of Nuclear Sciences – National Institute of the Republic of Serbia, University of Belgrade, Belgrade, Serbia*

<sup>2</sup>*Advanced Materials Department, Jožef Stefan Institute, Ljubljana, Slovenia*

<sup>3</sup>*nM2-Lab, Istituto di Struttura della Materia, CNR, Monterotondo Scalo (Roma) 00015, Italy*

<sup>4</sup>*Department of Chemistry and Industrial Chemistry, University of Genova, Genova, Italy*

In the last two decades, cobalt ferrite (CoFe<sub>2</sub>O<sub>4</sub>, CFO) has attracted extensive attention due to its applicability in data storage, catalysis, energy, environment, and in particular, biomedicine. To further extend applicability and improve understanding of fundamental processes, the present work investigates the influence of heteroatoms on physicochemical properties of CFO. Solvothermal method was used for designing a non-agglomerated particles with uniform morpho-structural properties. The physicochemical properties of Zn<sup>2+</sup> and Ga<sup>3+</sup> substituted CFO nanoparticles were examined (Co<sub>(1-x)</sub>Zn<sub>x</sub>Fe<sub>2</sub>O<sub>4</sub> and CoGa<sub>x</sub>Fe<sub>(2-x)</sub>O<sub>4</sub>; x=0, 0.1, 0.3 and 0.5). In order to isolate the contribution of heteroatoms, the synthesis condition were optimized to allow preparation of non-agglomerated particles with the narrow particle size and shape distribution, including the constant amount of capping agent. The X-ray diffraction (XRD) measurements confirmed the presence of pure cubic spinel phase in all samples, while the transmission electron microscopy (TEM) showed sphere-like nanoparticles with a mean diameter of 6±1 nm. The amount of adsorbed oleic acid on the surface of the nanoparticles, determined by thermogravimetric (TG) analysis, is 22-28 %, which indicates the formation of a complete monolayer of surfactant. The FT-IR analysis substantiated the presence of oleic acid on the surface of the nanoparticles and discovered its covalent bonding to the metal atoms. Substitution of host-atoms was also confirmed by Raman spectroscopy. Magnetic measurements revealed the influence of heteroatoms on saturation magnetization and magnetic anisotropy, showing for all the samples superparamagnetic behavior at room temperature. The substitution of Co<sup>2+</sup> and Fe<sup>3+</sup> ions with Zn<sup>2+</sup> and Ga<sup>3+</sup>, respectively, leads to the change in chemical composition and cationic distribution of CFO and consequently to variation of its magnetic properties that can be tuned for different applications.

## Heavily Pb-doped Ce-solid solutions

**Svetlana Butulija<sup>1</sup>, Jelena Maletaškić<sup>1</sup>, Bratislav Todorović<sup>2</sup>, Sanja Petrović<sup>2</sup>, Aleksandra Dapčević<sup>3</sup>, Branko Matović<sup>1</sup>**

<sup>1</sup>“Vinča“ Institute of Nuclear Sciences-National Institute of the Republic of Serbia, University of Belgrade, Mike Petrovića Alasa 12-14, Belgrade, Serbia

<sup>2</sup>Faculty of Technology of Leskovac, Bulevar Oslobođenja 124, Leskovac, Serbia

<sup>3</sup>Faculty of Technology and Metallurgy, Karnegijeva 4, Belgrade, Serbia

By *in situ* precipitation of nano-CeO<sub>2</sub> at room temperature, nanopowdered Ce<sub>1-x</sub>Pb<sub>x</sub>O<sub>2-δ</sub> solid solutions ( $x=5-30$ ) were synthesized. X-ray powder diffraction was used to study the lead solubility in ceria lattice. The results revealed that synthesized powders were single-phase with Pb solubility up to 30%. The thermal stability of the samples was investigated by thermal analyses (DTA-TG). All the solid solutions were stable at 600 °C, while at 900°C, samples doped up to 15% were stable. Also, pH-dependent resistance to leaching was estimated, and Pb releasing from ceria lattice decreased with increasing pH. The precipitation procedure provides a simple strategy for implementing Pb(II) into ceria lattice, widening the range of possible applications.

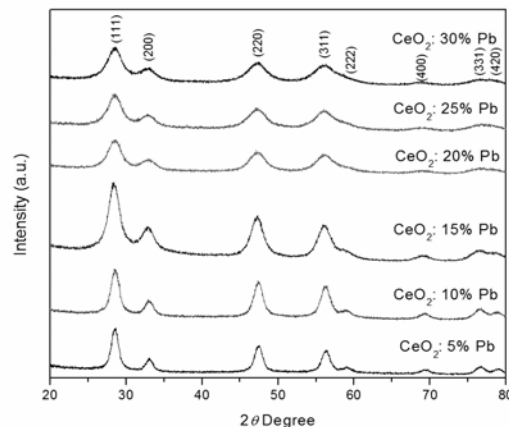


Figure 1. XRPD of Ce<sub>1-x</sub>Pb<sub>x</sub>O<sub>2-δ</sub> solid solutions ( $x=0.05-0.3$ )

## Crystal structure prediction of novel Cr<sub>2</sub>SiN<sub>4</sub> compound under extreme conditions

**Tamara Škundrić<sup>1,2</sup>, Dejan Zagorac<sup>1,2</sup>, Johann Christian Schön<sup>3</sup>, Jelena Zagorac<sup>1,2</sup>, Milan Pejić<sup>1,2</sup>, Dušica Jovanović<sup>1</sup>, Branko Matović<sup>1,2</sup>**

<sup>1</sup>*Materials Science Laboratory, Institute of Nuclear Sciences “Vinča”, University of Belgrade, Belgrade, Serbia*

<sup>2</sup>*Center for synthesis, processing and characterization of materials for application in the extreme conditions “CextremeLab”, Belgrade, Serbia*

<sup>3</sup>*Max Planck Institute for Solid State Research, Heisenberg str. 1, D-70569, Stuttgart, Germany*

Various machinery, especially equipment operating in harsh conditions such as marine environment, face severe damage during their usage. Hence, there is an urgent need for protective coatings, so they can work properly for a longer period. While transition metal nitride (TM-N) coatings are conventionally used for protection, CrN coatings are among the most widespread due to their outstanding properties. Nevertheless, because of its high friction coefficient, it is not appropriate for usage in extreme conditions. However, several previous studies have shown that the CrN complex can significantly improve its performance when Si is implemented. As it is suggested, the CrSiN coating is comprised of two phases, where the nanocrystalline CrN is embedded in the Si<sub>3</sub>N<sub>4</sub> amorphous matrix. Within this study, we conducted the first investigation of the bulk Cr<sub>2</sub>SiN<sub>4</sub> [1], since only CrSiN in thin films surveys were reported in previous experimental studies. In order to get insight into the structural stability of the possible phases existing in this system, we have performed global explorations of the energy landscape of the bulk Cr<sub>2</sub>SiN<sub>4</sub> using simulated annealing with an empirical potential [2,3], combined with data mining and the Primitive Cell approach for Atom Exchange (PCE) method [4]. Ab initio structural refinement confirmed several structure candidates on both the GGA-PBE and the LDA-PZ levels of calculation. The Global Optimization (GO) yielded five candidate structures possible to be observed at extreme conditions of temperature and/or pressure. The first of these structurally promising modifications appear in space group *P21/m* (no. 11) and is denoted as *nf1*-Cr<sub>2</sub>SiN<sub>4</sub>-type. The following structure candidate is referred to as *nf2*-Cr<sub>2</sub>SiN<sub>4</sub>-type, *nf3*-Cr<sub>2</sub>SiN<sub>4</sub>-type, *nf4*-Cr<sub>2</sub>SiN<sub>4</sub>-type, and the last modification within this group according to the total energy ranking is referred to as *nf5*-Cr<sub>2</sub>SiN<sub>4</sub>-type and crystallizes in space group *P-1* (no.2). After performing full structural optimization on the *ab initio* level using the GGA-PBE functional, data mining-based searches yielded several structure candidates likely to be detected at extreme conditions. The first modification is denoted as Ca<sub>2</sub>RuO<sub>4</sub>-type, followed by HgC<sub>2</sub>O<sub>4</sub>-like, Ca<sub>2</sub>IrO<sub>4</sub>-type, CaB<sub>2</sub>O<sub>4</sub>-like, and Mn<sub>2</sub>SnS<sub>4</sub>-type, respectively. Finally, the Primitive Cell for Atom Exchange (PCE) method generated three alternative structure candidates with two of them likely to be found at extreme conditions. Due to the exceptional properties of CrSiN coatings, presented in previous studies, further investigation of this ternary system is of crucial importance to determine the properties of these newly discovered phases as well as possibilities for industrial and technological applications.

### References

- [1] T.Škundrić, D. Zagorac, J. C. Schön, M. Pejić, B. Matović, Crystal Structure Prediction of the Novel Cr<sub>2</sub>SiN<sub>4</sub> Compound via Global Optimization, Data Mining, and the PCE Method. *Crystals* **2021**, *11*, 891.
- [2] Zagorac, D.; Schön, J.C.; Pentin, V.I.; Jansen, M. Structure prediction and energy landscape exploration in the zinc oxide system. *Processing and Application of Ceramics* **2011**, *5*, 73-78.
- [3] Zagorac, D.; Schön, J.; Zagorac, J.; Jansen, M. Prediction of structure candidates for zinc oxide as a function of pressure and investigation of their electronic properties. *Physical Review B* **2014**, *89*, 075201.
- [4] Zagorac, D.; Zagorac, J.; Schön, J.C.; Stojanović, N.; Matović, B. ZnO/ZnS (hetero) structures: ab initio investigations of polytypic behavior of mixed ZnO and ZnS compounds. *Acta Crystallographica Section B: Structural Science, Crystal Engineering and Materials* **2018**, *74*, 628-642.

## Mechanical and elastic properties of SiB<sub>6</sub>: Theoretical investigations through *ab initio* calculations

Tamara Škundrić<sup>1,2</sup>, Dejan Zagorac<sup>1,2</sup>, Aleksandra Zarubica<sup>3</sup>, Jelena Zagorac<sup>1,2</sup>  
Milan Pejić<sup>1,2</sup>, Dušica Jovanović<sup>2,3</sup>, Peter Tatarko<sup>4</sup>, Branko Matović<sup>1,2</sup>

<sup>1</sup>Materials Science Laboratory, Institute of Nuclear Sciences “Vinča”, University of Belgrade, Belgrade, Serbia

<sup>2</sup>Center for synthesis, processing and characterization of materials for application in the extreme conditions “CextremeLab”, Belgrade, Serbia

<sup>3</sup>Department of Chemistry, Faculty of Science and Mathematics, University of Niš, Niš, Serbia

<sup>4</sup>Institute of Inorganic Chemistry, Slovak Academy of Sciences, 845 36 Bratislava, Slovakia

Silicon borides are lightweight ceramics and are regarded as the most elusive refractory compounds. Owing to their remarkable features, represent very appealing industrial materials for research. Although silicon hexaboride is discovered at the beginning of the XX century, there is a surprisingly limited number of studies on the elastic and mechanical properties of SiB<sub>6</sub>, both in theory and experiment. In order to investigate the properties of this compound, first we have undertaken calculations using the *ab initio* minimization data mining approach [1,2] combined with the PCAE method [3], and several promising structure candidates have been found referred to as  $\alpha$ -SiB<sub>6</sub>,  $\beta$ -SiB<sub>6</sub>, and  $\gamma$ -SiB<sub>6</sub> modifications. For these most relevant modifications, elastic constants  $C_{ij}$  have been calculated using GGA-PBE and LDA-PZ approach and were compared to previous theoretical data. Cubic  $\gamma$ -SiB<sub>6</sub> modification has only three independent elastic constants which are in very good agreement with available theoretical data. Using the elastic constants, mechanical stability was investigated and the results suggest instability in the cubic  $\gamma$ -SiB<sub>6</sub> structure, which is also in agreement with previous theoretical studies. Elastic constants for the  $\alpha$ -SiB<sub>6</sub> phase are reported for the first time and indicate the mechanical stability of this phase. The last one, the  $\beta$ -SiB<sub>6</sub> phase has a lower orthorhombic symmetry and a larger number of independent elastic constants that were calculated using both the LDA and GGA approach and the results agree well with previous studies. According to the calculated results, the  $\beta$  phase is mechanically stable that also concurs with previous studies. Within this study, the bulk modulus B, Shear modulus K, Young's modulus E, Poisson's ratio  $\nu$ , and Pugh's criterion B/K for these modifications have been calculated [4]. According to the calculated Poisson's ratio and Pugh's criterion (B/K) using both GGA and LDA methods, it can be assumed that the  $\beta$ -SiB<sub>6</sub> phase will have a brittle character, while  $\alpha$  and  $\gamma$ -phase seem to be ductile. As it was suggested from several earlier studies that SiB<sub>6</sub> has excellent potential as high-temperature material, and it has been considered as a material with the ability to operate in extreme environments, further research of this compound is required. Investigation in detail of these newly discovered phases and their properties is of great importance in order to find new possibilities for future industrial and technological applications.

### References

- [1] Zagorac, D.; Schön, J.C.; Jansen, M. Identification of promising chemical systems for the synthesis of new materials structure types: An *ab initio* minimization data mining approach. *Processing and Application of Ceramics* **2013**, *7*, 37-41.
- [2] Zagorac, J.; Zagorac, D.; Zarubica, A.; Schon, J.C.; Djuris, K.; Matovic, B. Prediction of possible CaMnO<sub>3</sub> modifications using an *ab initio* minimization data-mining approach. *Acta Crystallographica Section B* **2014**, *70*, 809-819, doi:doi:10.1107/S2052520614013122.
- [3] Zagorac, D.; Zagorac, J.; Schön, J.C.; Stojanović, N.; Matović, B. ZnO/ZnS (hetero) structures: *ab initio* investigations of polytypic behavior of mixed ZnO and ZnS compounds. *Acta Crystallographica Section B: Structural Science, Crystal Engineering and Materials* **2018**, *74*, 628-642.
- [4] Škundrić, T.; Matović, B.; Zarubica, A.; Zagorac, J.; Tatarko, P.; Zagorac, D. Structure Prediction and Mechanical Properties of Silicon Hexaboride on *Ab Initio* Level. *Materials* **2021**, *14*, 7887.

## Damage to a tube of output reheater due to gas corrosion

**Vladimir Pavkov<sup>1</sup>, Gordana Bakić<sup>2</sup>, Vesna Maksimović<sup>1</sup>, Miloš Đukić<sup>2</sup>, Bratislav Rajičić<sup>2</sup>,  
Aleksandar Maslarević<sup>3</sup>, Branko Matović<sup>1</sup>**

<sup>1</sup>*Vinca Institute of Nuclear Sciences, University of Belgrade, Belgrade, Serbia*

<sup>2</sup>*Faculty of Mechanical Engineering, University of Belgrade, Belgrade, Serbia*

<sup>3</sup>*Innovation center Faculty of Mechanical Engineering, University of Belgrade, Belgrade, Serbia*

One of the most responsible elements of modern steam boilers are steam superheaters and reheaters. These heating surfaces are inside the boiler chamber and consist of tubes connected to the inlet and outlet header. Due to the complexity of service conditions, boiler tubes are exposed to processes of gradual degradation, and consequently a decrease in operating performance and reliability.

In the operation of thermal power plants, irreversible metal losses resulting from corrosion can cause tube failure and plant outage. Considering the loss of materials, gas corrosion in the dry gas atmosphere due to the high temperature is of great importance. Gas corrosion can be expressed in the boiler tubing system due to the presence of sulfur compounds in the flue gases. For this reason, it must be borne in mind that the outer surface of a tube of final reheater has different damage mechanisms during operation, and one of them is gas corrosion. Gas corrosion causes material loss and provides a site for crack initiation and propagation, which can compromise the integrity of the pressure vessel.

In this paper, a tube of a final reheater from a 210 MW power plant was tested. The tube was in service 200,000 h at a working temperature of 540 °C and a maximum working pressure of 4.6 MPa. The tube is made of low alloy Cr-Mo-V steel, class 12H1MF (GOST). After long-term service, a rough surface and loss of the material in the form of a crater were observed on the outer surface of the tube as a result of the effect of gas corrosion, together with the change of microstructure due to elevated service temperature. The measured depth of damage to the tube is 120 µm. The presence of gas corrosion on the tube was confirmed and measured by an optical microscope, Figure 1.

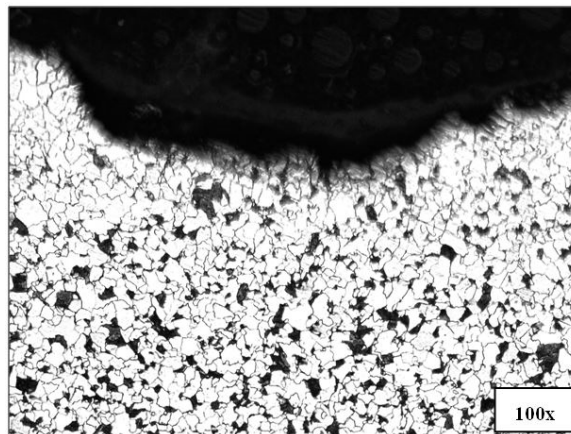


Figure 1. The microstructure of an outer surface of the reheater tube after 200,000 h of service

## **Influence of host lattice on luminescence properties of up-conversion $\text{Ln}_2\text{MoO}_6$ (Ln=Y, Gd) powders co-doped with $\text{Er}^{3+}/\text{Yb}^{3+}$ synthesised at high temperatures**

**Nadežda Radmilović, Tijana Stamenković, Vesna Lojpur**

*Vinča Institute of Nuclear Sciences, National Institute of the Republic of Serbia, P.O. Box 522,  
11001 Belgrade, University of Belgrade, Serbia*

Luminescent materials emit radiation when exposed to various types of excitation (ultraviolet radiation, X-rays, electron beam, etc.) and can be comprised of a host lattice with dopant as an activator. One of the extensively investigated luminescent materials is monoclinic  $\text{Ln}_2\text{MoO}_6$  due to its high thermal stability. In this study, we investigated  $\text{Ln}_2\text{MoO}_6$  with different concentrations of  $\text{Er}^{3+}/\text{Yb}^{3+}$  concentrations synthesized at temperatures up to  $1200^\circ\text{C}$ . The obtained powders were examined by X-ray diffraction (XRD), scanning electron microscopy (SEM), transmission electron microscopy (TEM) and photoluminescence spectroscopy (PL). The results revealed that all powders are single phase  $\text{Ln}_2\text{MoO}_6$ , with particle size in the nano range at lower treatment temperatures (up to  $800^\circ\text{C}$ ) and in the micro range at higher calcination temperatures (up to  $1200^\circ\text{C}$ ). Both  $\text{Y}_2\text{MoO}_6 : \text{Yb}^{3+}/\text{Er}^{3+}$  and  $\text{Gd}_2\text{MoO}_6 : \text{Yb}^{3+}/\text{Er}^{3+}$  show double emitting luminescence two green emission bands at 525 and 546 nm ( $^2\text{H}_{11/2}, ^4\text{S}_{3/2} \rightarrow ^4\text{I}_{15/2}$ ) as well as a red emission band at 657 nm ( $^4\text{F}_{9/2} \rightarrow ^4\text{I}_{15/2}$ ). It can be concluded that increase of  $\text{Yb}^{3+}$  concentration leads to change of the green to red ratio showing the ability for fine-tuning of the color output.

## AUTHOR INDEX

Bajuk-Bogdanović Danica 36  
Bakić Gordana 25, 26, 61  
Baranchikov Alexander 47  
Bermejo Raul 37  
Boháč Peter 23  
Butulija Svetlana 43, 46, 58  
Čebela Maria 50, 51, 52  
Chlup Zdeněk 18,  
Ciganović Jovan 20  
Ćurković Lidija 49, 55  
Cvijović-Alagić Ivana 20, 43  
Czímerová Adriana 23  
Daneu Nina 36  
Dapčević Aleksandra 58  
Devečerski Aleksandar 56  
Dlouhý Ivo 18, 28  
Đorđe Petrović 56  
Đukić Miloš 25, 26, 61  
Egerić Marija 56  
Emory Joshua 30  
Erčić Jelena 40, 43, 47, 51  
Fedor Ján 27  
Fimml Wolfgang 37  
Fonović Matej 33  
Gabelica Ivana 49  
Gajtko Olga 47  
Grasso Salvatore 28  
Gruber Manuel 37  
Grujičić Marija 57  
Gubarevich Anna 30  
Hanzel Ondrej 27, 28, 43  
Harrer Walter 37  
Hičák Michal 18, 24  
Hnatko Miroslav 24  
Ivanov Vladimir 47  
Ivanova Olga 47  
Janković Bojan 46  
Jelenković Branislav 38  
Jelić Marko 57  
Jovanović Dušica 34, 43, 44, 45, 48, 53, 54, 59, 60  
Jovanović Sonja 57  
Jovanović Zoran 36



Kapuran Đorđe 35  
Kim Young-Wook 27  
Knežević Zoran 33  
Kostoglou Nikolaos 39  
Kovalčíková Alexandra 18, 28  
Kumar Ravi 19  
Kumrić Ksenija 56  
Laketić Slađana 20  
Lenčes Zoltán 23, 24, 27  
Lisnichuk Maksym 43  
Liverić Lovro 33  
Lojpur Vesna 50, 51, 52, 62  
Maček-Kržmanc Marjeta 57  
Maksimović Vesna 25, 31, 61  
Maletaškić Jelena 30, 40, 58  
Maslarević Aleksandar 25, 61  
Matović Branko 18, 29, 32, 34, 39, 40, 43, 44, 45, 46, 47, 48, 53, 54, 58, 59, 60, 61  
Matović Ljiljana 56  
Milosevic Nenad 25  
Momčilović Miloš 20  
Mravik Željko 36  
Nengqing Liao 30  
Nikolic Marko 29  
Nikolić Nebojša 31  
Olejniczak Andrzej 36  
Omerašević Mia 56  
Pavkov Vladimir 25, 61  
Peddis Davide 57  
Pejić Milan 34, 43, 45, 48, 53, 54, 59, 60  
Perisic Jovana 26  
Petrisková Patrícia 23  
Petrović Sanja 58  
Prekajski Đorđević Marija 29, 40, 50  
Premović Pavle I. 42  
Radmilović Nadežda 50, 51, 62  
Radwan Mohamed 23  
Rajičić Bratislav 25, 26, 61  
Rakin Marko 20  
Randelović Marjan 32  
Rebholz Claus 39  
Rončević Sanda 49  
Ropuš Ivana 49  
Rosić Milena 52  
Rumyantseva Marina 47

Šajgalík Pavol 23, 24, 27  
Schön Christian J. 34, 59  
Sedlák Richard 43  
Sedmak Aleksandar 26  
Shekunova Taisiya 47  
Sijacki Zeravci Vera 26  
Škundrić Tamara 34, 43, 45, 48, 53, 54, 59, 60  
Skuratov Vladimir 36  
Spreitzer Matjaž 36  
Spreitzer Matjaž 57  
Stajcic Ivana 46  
Stamenković Tijana 50, 51, 62  
Stoiljković Milovan 35, 46  
Stojanović Sreten B. 42  
Stojiljković Dragan T. 42  
Subasri R. 40  
Tatarko Peter 18, 28, 43, 60  
Tatarková Monika 18,  
Tilz Anton 37  
Todorović Bratislav 42, 58  
Tomašić Neven 33  
Ünsal Hakan 18, 28  
Veličković Suzana 35, 46  
Veljković Filip 35, 46  
Veljović Đorđe 20  
Vujasin Radojka 56  
Vukomanović Marija 57  
Vukšić Milan 55  
Wasim Muhammad 26  
Wimmer Andreas 37  
Yang Lili 47  
Yorov Khursand 47  
Yoshida Katsumi 30  
Zagorac Dejan 21, 34, 43, 44, 45, 47, 48, 53, 54, 59, 60  
Zagorac Jelena 34, 43, 44, 45, 48, 53, 54, 59, 60  
Zarubica Aleksandra 32, 60  
Žmak Irena 55

**ISBN 978-86-7306-158-0**